Development of microsystem for water-in-oil droplet generation

Linus Jonsson

June 2014

LUND
UNIVERSITY

Master Thesis

Faculty of Engineering, LTH
Department of Biomedical Engineering

Supervisor: Maria Tenje

Abstract

Droplet microfluidics has shown great potential for biological assays, chemical reactions and polymer emulsions. High stability allow the droplets to work as stable and isolated reactors that open up for parallel and serial reactions where each droplet can be screened individually. This results in assays with increased through-put, faster reactions with better response and low costs (due to small amounts of sample used). The purpose was to fabricate such systems in PDMS and glass, establish stable droplet generation where droplet volumes range from picoliter to nanoliter and to suggest further improvement. This thesis aims to examine water-in-oil droplet generation in microfluidic systems; where a fabrication method is optimized and functional devices are manufactured. The thesis presents droplet formation in microfluidic channels by theoretical simulations and by experimental work. Different droplet regimes are found in both theoretical simulations and in experimental work by altering flow rates and flow rate ratios of two immiscible fluids. Stable and monodisperse droplets are generated with low dispersity ($1-3\%$). Further, the results show that the droplet size is dependent on the flow rates and flow rate ratios of the two fluids, channel dimensions and surfactant concentrations.

Keywords: Microfluidics, Microfabrication, Fluid dynamics, Interfacial tension, Shear rate, Rayleigh-Plateau instability, Simulations, Droplets

Preface

Thesis Background
As the last part of the master degree in Engineering Nanoscience I have done a master thesis at the department of Biomedical Engineering (BME) at the Faculty of engineering, LTH, Lund University. The thesis was given as one of many proposals to me after a meeting with Johan Nilsson, prefect of the BME department. I decided to take this thesis after a second meeting with Johan Nilsson and Maria Tenje, Assistant Professor at the department. At that meeting it was decided that Maria Tenje would be my supervisor, Johan Nilsson my secondary supervisor and Andreas Lenshof my examiner of the thesis and presentation.

Acknowledgement
I would like to thank my supervisor Maria Tenje for all support in my work with my master thesis. M. Tenje have introduced me to the department, been very supportive and given me valuable feedback as my work proceeded and helped me with this thesis. I'm also very thankful that she gave me the opportunity to participate in the MicroNano System Workshop 2014 (MSW 2014) at Uppsala University. I would also like to thank my secondary supervisor, J. Nilsson, for his support and feedback on my work. In addition, many thanks to all employees at the BME department for their contribution to my work, such as helping me with practical issues, feedback, lending me material, guidance and more.

I also would like to thank my family and friends for their support and for paying interest in my studies and the assistance given when my motivation has been low. At last I have to say that I've been through a few ups and downs during my master thesis, but I would like to quote my former head coach in my American Football team.

> *Nothing is ever as bad as it looks. Nothing is ever as good as it looks. The truth lies somewhere in between.*
> - George Contreras, 2010

Contents

Chapter 1

Introduction

1.1 Background

In recent years has microfluidics grown into a major scientific and interesting technology that manipulate and process small amounts of fluids (10^{-9} to 10^{-18} litres) in channels with dimensions of few to hundreds micrometer [1]. The microfluidic technology gives many benefits compared to macro systems; due to the small volumes used the amount of reagents and solvents are drastically reduced (from millilitres to micro- and nanolitres) and thus, the time for mixing by diffusion is decreased (from hours to seconds or less). Due to the low volumes and quick mixing, reactions occur faster with better response. Parallel and serial reactions can be implied, which gives microfluidic systems high through-put. This technology has opened up a wide array of applications that utilize microfluidics; from drug delivery [2] to point-of-care diagnostic chips to organic synthesis [3], cell analysis [4] and microreactors [5, 6] and more. The minimizing of experiments and analysis to the micro- and nanoscale performed on small and single devices or chips is referred as 'lab-on-a-chip' [7].

With the advances achieved in the technology of fabrication on the microscale there are multiple ways to design and fabricate microfluidic systems [8]. One common method is soft lithography, where a substrate, usually Silicon or glass, coated by a photosensitive polymer, commonly used is the negative resist SU-8, which will be patterned by photolithography. After the development of the exposed resist, which either removes the exposed or unexposed resist, results in a topographic pattern on the substrate. A rubber, most notably Polydimethylsiloxane (PDMS), is then poured on the substrate that after the curing process yields an inverse replica of the pattern. The rubber slab is then detached and bonded to a glass wafer or another PDMS slab that result in micrometer wide microfluidic channels [9–11], see figure 4.4.

The majority of works performed in the microfluidic field utilize one continuous fluid that travels through the fabricated channel. However, if two immiscible fluids would be used in a system plugs or droplets can be generated where one fluid is isolated in the other one. The isolated plugs or droplets created are made of a "dispersed"-phase travelling in a "continuous"-phase. A simple example is vapour bubbles in water or water-in-oil droplets. At the microscale these droplets have extremely small volumes (10^{-9} to 10^{-12} litres) which results that the diffusion distance is further decreased, thereby increasing the mixing rate for chemical and biological reactions. The use of droplet microfluidics allows individual screening of droplets, parallel and serial chemical [12] and biological reactions [13], which results in high throughput devices as well as keeping the costs low due to the small volumes required [14].

1.2 Purpose

The research at the department of Biomedical Engineering (BME) at Lund Faculty of Engineering, LTH, have so far only involved water-based solutions and want to extend their research to involve droplet based microfluidics due to its enormous potential. They are interested in exploring the technology of water-in-oil (W/O) droplet microfluidics and are looking to establish the technology at their department. In the longer turn they want to incorporate this technology with their current research on integrated ultrasound - acoustophoresis.

The tasks in the project are to dig into the state-of-art literature of droplet microfluidics, design and fabricate droplet generating systems in PDMS and glass, then evaluate the performance and suggest further improvements.

1.3 Related Works

As a motivation or to give a more clear view of why microdroplets in microsystems can be important for scientific research comes here a small section presenting studies that utilize two immiscible fluids in their microsystems.

Two examples of applications involving droplet microfluidics are studies where single emulsions are used for gene delivery and gene therapy. The first example is a study where they used water droplets, formed in a T-junction, as carriers for DNA plasmids to be transfected into COS-7 cells. In addition to a fabricated T-junction they used a pneumatic membrane chamber inte-

grated near the intersection of the T-junction once filled with compressed air could fine-tune the droplet size [15]. With higher applied are pressure smaller droplets were generated. They found that the size of the emulsion droplets played an important role on the efficiency in gene delivery, meaning that the smaller the droplets the higher transfection activity. The other example is a study where cells and plasmid DNA are fused together in droplets flowing in oil in a microfluidic device. The cells are then transfected by plasmid DNA by electroporation when the droplets flowed through a pair of integrated microelectrodes. They demonstrated the delivery of enhanced green fluorescent protein (EGFP) plasmids into Chinese hamster ovary (CHO) cells when a constant voltage was applied to the electrodes [16].

Another example of study involving droplets is done by Kubo *et al.*. They present the preparation of molecular imprinted polymer (MIP) particles for selective binding for the pesticide atrazine [17]. Droplets containing atrazine, methacrylic acid (MMA) and photoinitiator are generated in a Y-shaped variation of a T-junction in an aqueous continuous phase. Monodisperse droplets were formed by UV radiation that yield MIP particles with selective binding to atrazine. MIP particles with selective binding to a pesticide can be used in chemical detection and for food safety monitoring.

1.4 Overview of the Thesis

The thesis is divided into chapters that follows this Introduction chapter. The second chapter explains briefly theory and other fundamentals principles of microfluidics and microdroplet formation. The third chapter describes the fabrication methods and simulations. The fourth chapter present the results followed by discussion chapter - both with aspect of the fabrication, simulations and experimental results. After that, comes a conclusion of the thesis and a popular scientific summary. Lastly comes the Bibliography and Appendices.

Chapter 2

Theory & Fundamentals

2.1 An Overview of Microfluidics

This section present a short introduction to microfluidics, covering some basic underlying concepts. A more extensive theoretical and mathematical approach to learn microfluidics can be read in [18].

2.1.1 What is a fluid?

Microfluidics involves the behaviour of fluids when applied in the submillimeter scale. Because, fluids do behave differently in the microscale than in macroscale. However, before digging into the theory deeper one must know what a fluid is. The commonly used definition of a fluid is "a substance that continually deforms (flows) under an applied shear (tangential) stress" [19]. Fluids are most commonly known as liquids but fluids are not only liquids, as many believe, but also includes gases and plasmas. Fluids display properties such as the ability to deform continuously (or only slightly due to its viscosity) under external force and the ability to flow (to take the shape of the container). Fluids can also be considered as a continuum or discrete fluid particles. In the continuum hypothesis, the fluid macroscopic properties are said to be the same as if the fluid was perfectly continuous instead of consisting of discrete particles. For a volume of fluid, physical quantities, e.g. mass, momentum and energy, are considered to be the sum of all quantities for the molecules building up the volume [18].

One of the most important aspects of fluids in microsystems is the scaling factor that causes surface properties to dominate over volume properties, e.g. surface tension, evaporation and viscosity will govern gravity and inertia. This is due to the increasing surface-to-volume ratio as the size of a system

or object decreases:

$$\frac{surface}{volume} \propto \frac{l^2}{l^3} = l^{-1}, \lim_{l \to 0} l^{-1} = \infty \tag{2.1}$$

One example of different behaviour of a fluid in the microscale compared to macroscale is the laminar flow that occurs in microsystems. In our everyday life we see the flow of liquids as turbulent and chaotic. An example is when one mixes two liquids. The mixing occurs randomly and the liquids flow into each other. In contrast, laminar flow is a more organized and well ordered flow, where a fluid will flow laminated, a streamline flow where the streams flow next to each other and mixing occurs only due to diffusion. What determines if the flow is turbulent or laminar? The Navier-Stokes equations are a set of equations that describe the motion of a fluid and can be used to determine if the flow is turbulent or laminar. More of this will be discussed in the Fluid Dynamics section.

2.1.2 Newtonian and non-Newtonian Fluids

Normally, fluids are said to be *Newtonian* because their viscosity, μ, vary very little in viscous stress tensor and can therefore be taken as constants. Basically, their viscosity is constant as the rate of strain changes. The contradicting, the *non-Newtonian* fluids, change their viscosity depending on the rate of strain. This is due to the fact that the fluid contains large deformable molecules or particles that can be extended at increased shear stress, thus leading to a decrease or increase in viscosity [18]. Examples of non-Newtonian fluids are blood, starch and some polymers. In this work, we have only worked with Newtonian fludis.

2.1.3 Fluid Dynamics

The behaviour and motion of fluids can be described by the Navier-Stokes equations, which are based on a couple of partial equations. The first equation is the *conservation of mass*, which states for a fluid in steady-state, that the rate of mass entering a system is equal to the rate of mass leaving the system. The second equation is the *conservation of momentum*, which states that in a closed system (no exchange of any matter with the outside and no outside forces acting) is the total momentum constant. The third equation *conservation of angular momentum*, which states that when no outer torque acts on an object or closed system, no change of angular momentum can occur. The fourth and last equation is the *conservation of energy*, which states that the total energy of an isolated system (a system where no matter or energy can pass) cannot change. The derivation of the Navier-Stokes equations

will not be presented in this thesis, but can be read in [18]. The final form of the equations, for incompressible Newtonian fluids, is presented below:

$$\rho\left[\frac{\partial \mathbf{v}}{\partial t} + (\mathbf{v}\cdot\nabla)\mathbf{v}\right] = -\nabla p + \mu\nabla^2\mathbf{u} + \mathbf{F} \tag{2.2}$$

where $\mathbf{v}$ is the flow velocity, ρ is the fluid density, p is the pressure, μ is the dynamic viscosity and $\mathbf{F}$ is other outer forces.

From Eq. 2.2 one can determine which forces that are governing for a specific system. At high flow rates and long characteristic length scales the inertial and mass movement dominates and the flow will be turbulent, while at low flow rates viscous forces dominate and the flow will be laminar.

Laminar vs. Turbulent Flow

In microsystems, where Reynolds numbers are very small, or other systems where the dynamic viscosity is dominant the fluid flow is said to be laminar, given by the Navier-Stokes equations, Eq. 2.2. Laminar flow or streamline flow is when the fluid flows in parallel layers, without any interference between the layers. The parallel layers are "sliding" on each other, compare when playing cards are sliding on one another. The streamline flow is ordered in lines parallel to the channel walls. Lateral mixing for particles in the fluid can only occur due to diffusion. The opposite is the turbulent flow, characterized by chaotic flows. Here mixing occurs due the turbulent flow where the momentum convection is high and pressure and velocity can change through-out the fluid. Laminar flow will also form a parabolic flow profile; where the highest velocities of the flow is in the middle of the channel and the lowest flows next to the walls. Sometimes, for simplification, the flow velocity next to the wall is set to be zero. See figure 2.1 for a schematic visualization of the laminar and turbulent flows.

2.1.4 Dimensionless Numbers

For fluids in microsystems there exist many physical phenomena where *dimensionless numbers* can be used to determine which of these phenomena that takes place in the system. This applies both for single and multiphase microfluidics. The dimensionless numbers are relative numbers and are calculated by the ratio of different parameters and the numbers gives a hint on what phenomena dominates in the system [21]. Example, a fluid flow is said to flow laminar if Reynolds number is low ($Re < 1500$) but to be turbulent if the number is high ($Re > 1500$) [19]. Below are a few dimensionless numbers discussed, which are often mentioned in droplet microfluidics.

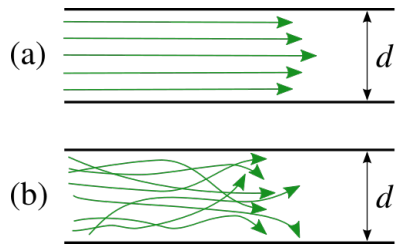

Figure 2.1: Laminar flow (a) is a layer-ordered flow that assumes an parabolic flow profile; highest velocity in the middle and lowest at the walls. Turbulent flow (b) is considered to be chaotic flow where e.g. velocity can change trough-out the flow. Figure from [20].

Reynolds Number

One of the most mentioned dimensionless number is the Reynolds number (Re) and gives the ratio of inertial forces to viscous forces. The Reynolds number can be derived from the Navier-Stokes equations, Eq. 2.2, by neglecting the non-linear term $\rho(\mathbf{v} \cdot \nabla \mathbf{v})$ (which can be done at low flow velocities) and making the equation dimensionless (replace all physical variables in units of the characteristic length scale) [18]. The Reynolds number is defined as:

$$Re = \frac{\rho D_H v}{\mu} \tag{2.3}$$

where ρ is the density, D_H is the hydraulic diameter or characteristic length, v is the mean velocity of the fluid and μ is the dynamic viscosity. At low Reynolds number the viscous forces tend to dominate over the inertial forces, resulting in linear flows (laminar flow) [21]. The hydraulic diameter is a term used when handling flows in noncircular channels. Basically, the hydraulic diameter is used so one can calculate different entities, such as Reynolds number, as if the channel of interest were circular. It is defined as:

$$D_H = \frac{4A}{P} \tag{2.4}$$

where A is the cross-sectional area and P the wetted perimeter of the cross-section. Often, microsystem deals with very small Reynolds number ($10^{-6} - 1$) [22], and the flow can be said to be laminar in most microfluidic devices.

Capillary Number

For *miscible* fluids, parallel streams are assumed to flow side by side along each other and particles can diffuse from one stream into the adjacent stream. But for *immiscible* fluids a surface tension (also called interfacial tension)

tends to separate the fluids. The capillary number represent the ratio of viscous forces to surface tension acting across an interface of two immiscible fluids, such as liquid and air or water and oil. The viscous forces tend to deform the surface while the surface tension tends to minimize the surface [21]. The capillary number is above other dimensionless numbers important for the droplet formation in microfluidics, and is defined as:

$$Ca = \frac{\mu v}{\gamma} \tag{2.5}$$

where μ is the viscosity of the continuous phase, v is the velocity of the continuous phase and γ is the surface or interfacial tension between the two phases.

Weber Number

Another dimensionless number that is useful when studying multiphase flows, except from the capillary number, is the Weber number. The number represents the ratio of the inertial forces to surface tension. The Weber number is defined as:

$$We = Re * Ca = \frac{\rho v^2 L}{\gamma} \tag{2.6}$$

where ρ is the density, v mean velocity of the fluid, L is the characteristic length scale (typical the droplet diameter) and γ is the surface or interfacial tension between the two phases.

Bond Number

The Bond number is dimensionless number that also can be used in multiphase fluidics. It evaluates the gravitational forces to interfacial tension, and is defined as:

$$Bo = \frac{\rho g L^2}{\gamma} \tag{2.7}$$

where ρ is the density or density difference between fluids, g is the gravity, L is the characteristic length scale (typical the droplet diameter or radius of a capillary tube) and γ is the surface or interfacial tension between the two phases.

Flow Rate Ratio

Another number intresting in microfluidic two-phase flows is the flow rate ratio between the continuous phase and the discrete phase and can be expressed as a fraction between the two rates:

$$\varphi = \frac{Q_{dispersed}}{Q_{continuous}} \tag{2.8}$$

2.1.5 Surface Tension

Surface tension, also called interfacial tension, is an important phenomena for fluids and depends on the two materials on each side of an interface. The definition of surface tension is Gibbs free energy per area for a fixed pressure and temperature [18] :

$$\gamma \equiv \left(\frac{\partial G}{\partial A}\right)_{p,T} \tag{2.9}$$

The Si unit for surface tension is

$$[\gamma] = Jm^{-2} = Nm^{-1} = Pa \cdot m \tag{2.10}$$

To explain interfacial tension consider a liquid droplet in a vapour. The liquid molecules in the droplet interact with each other, due to intermolecular interactions, see figure 2.2. Molecules in the bulk of the droplet can interact with neighbouring molecules in all directions, causing balanced interactions. However, molecules at the surface can only interact with molecules inwards, causing unbalanced interactions. This unbalanced interaction results in a higher energy for the surface molecules, thus the droplet tends to lower its surface area by curving its surface, since that will be more energetically favourable [22]. Surface tension is especially important in multiphase systems, which will be more discussed in the next chapter, Droplet Formation.

The contact angle of a liquid droplet on a substrate indicates if the surface of the substrate is hydrophilic ($\theta_C < 90°$) or hydrophobic ($\theta_C > 90°$); where Young's equation, Eq. 2.11, can be used to calculate that quantity:

$$0 = \gamma_{SG} - \gamma_{SL} - \gamma_{LG} \cdot \theta_C \tag{2.11}$$

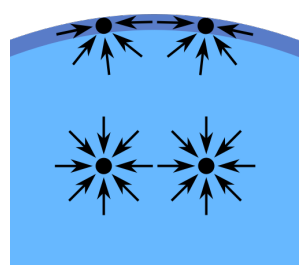

Figure 2.2: Schematic illustration of intermolecular interactions in bulk and at interface of a liquid droplet in vapour. Figure from [23].

This equation also involves the interfacial tension quantity between liquid and vapour, and the equation is a matter of thermodynamic equilibrium between the three phases; solid, liquid and vapour, see figure 2.3.

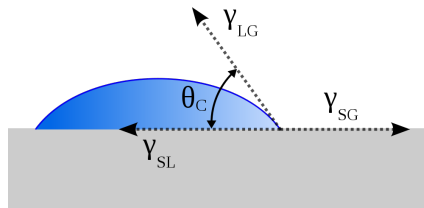

Figure 2.3: Schematic illustration of a liquid droplet on a substrate. Quantities from Young's equation; θ_C gives the equilibrium contact angle, γ_{SG} the solid-vapor interfacial energy, γ_{SL} the solid-liquid interfacial energy and γ_{LG} the liquid-vapor interfacial energy (i.e. surface tension). Figure from [24].

2.2 Droplet Formation

As said before, droplet generation of one fluid in a second immiscible fluid is useful in a wide range of applications, for research, polymeric emulsions and as chemical and biological reactors. The ability to control monodisperse droplet formation, both in aspect of droplet size and generation rate are important for achieving their intended functions. However, there are numerous approaches to create isolated droplets in the micro- and nanoscale, and several regimes where droplet breakup occurs. There are three typical device geometries used for generating both isolated droplets and plugs. This chapter will briefly cover the fundamentals of droplet formation.

2.2.1 Rayleigh-Plateau Instability

One important phenomena in fluid dynamics concerning fluid thread breakup is the Rayleigh-Plateau instability, which is interesting in droplet formation in two-phase systems. Consider a thread or stream of a fluid inside another fluid (liquid or gas) that by elongation starts to form larger nodules of fluid. This is due to tiny perturbation within the stream of the dispersed fluid that resolves into sinusoidal shape; some parts of the thread will grow with time and some will decay. Two immiscible fluids in microfluidics will, at a specific flow regime, form a jet or thread of a dispersed phase inside a continuous phase and will develop these sinusoidal undulations, due to the perturbations in the fluid. The undulations grow larger and will finally break the jet into droplets, see figure 2.5 (c), this phenomena is referred to

as the Rayleigh-Plateau instability [25, 26]. The volume in the jet is split into droplets that will contain the same volume, but at lower surface energy. This behaviour can be seen in some droplet breakup regimes in droplet generating systems. In addition to the formed droplet one or several much smaller satellite droplets, also called secondary droplets, can follow that main droplet. These satellite droplets are formed in the breakup process due to recoil disturbance when the main droplet is separated from the jet [26]. This phenomena is often unwanted since many applications depends on precise formation of monodipserse droplets.

2.2.2 Droplet Generating Systems

Most systems generating droplets, where droplets can range from picoliters to microliters, are usually achieved through passive techniques where a dispersed phase encounters a continuous phase using syringe pumps. At the interface of the two phases the flow field deforms the interface and induce instabilities that promote droplet break-up [27]. There are mainly three distinct approaches to generate uniform droplets; breakup in T-junctions, breakup in co-flowing streams and breakup in flow-focusing devices [22]. These approaches for droplet breakup can be designed and fabricated in different ways, but often result in systems generating stable and monodisperse droplets. However, it is not only the geometry of the device that determines the size of the droplets. Factors such as the viscosities of the phases, use of surfactants, hydrophobicity of the channel walls and interfacial tension also affect the flow field that will affect the droplet breakup or pinch off [14, 22, 27]. Droplet polydispersity in these systems, which gives a number of the size deviation - defined as the standard deviation of the size distribution divided by the mean droplet size - can be as low as 1 to 3% [27]. In the experimental work the T-junction and flow-focusing approach were tested.

T-junctions

T-junctions are the most used device geometries for the production of plugs and droplets in two-phase systems. It was first studied by Thorsen *et al.* [28] where they generated monodisperse isolated droplets at frequency of 20-80 Hz, using pressure controlled flows.

Droplet Regimes for T-junctions

De Menech *et al.* identified three distinct flow regimes that result in droplet formation by numerical simulation studies; squeezing, dripping and jetting [29]. At low capillary number the droplet formation is in the squeezing regime. In this regime the dispersed phase goes into the continuous phase

and blocks almost the entire cross-section of the main channel. The breakup process occurs when the pressure upstream of the droplet increases, thus, the continuous phase starts to squeeze the neck of the dispersed phase [27, 29]. At high capillary numbers the droplet formation goes into the dripping regime. Here the dispersed phase will only partially fill the main duct and when the action of viscous shear stress overcomes the interfacial tension droplet breakup occurs. Additionally, the breakup point moves downstream of the T-junction corner and result in smaller droplets. To change the volume of the droplets one can alter the fluid flow rates, channel widths or changing the relative viscosities for the two phases [14, 29]. The third regime, called the jetting regime, occurs at even higher capillary number. The transition from dripping to jetting is characterized when the breakup point progressively moves downstream from cycle to cycle, eventually leading to a formed jet [29]. Because of the very high capillary number required for the jetting regime this regime is not very used in microfluidic applications. These regimes are also presented in a study by Liu and Zhang [30], where they showed the different droplet regimes at different capillary numbers and flow rate ratios, performed by numerical simulations, see figure 2.4.

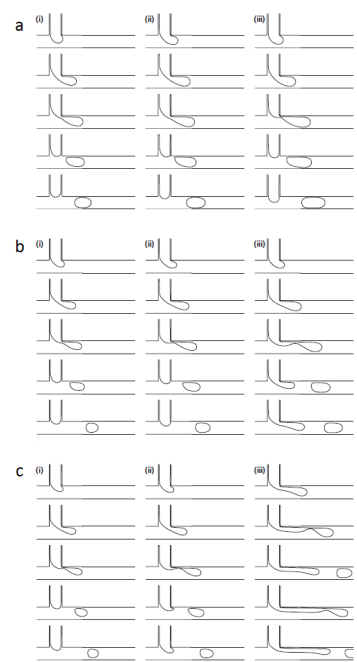

Figure 2.4: Numerical simulations show the dependency of capillary number and flow rate ratio for the three regimes: squeezing, dripping and jetting. *Ca* is (a) 0.006, (b) 0.032 and (c) 0.056; flow rate ratio φ is (i) 1/8, (ii) 1/4 and (iii) 1/2. Figure is from ref. [30].

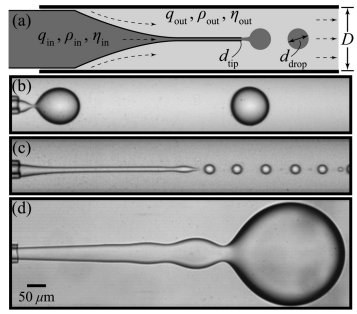

Figure 2.5: Figure showing the different regimes for drop formation in a co-flowing setup. (a) shows device geometry, (b) dripping regime, (c) jetting regime with narrowing jet and (d) jetting regime with widening jet. Figure is from ref. [31].

Co-flowing

The second approach is to apply a geometry that opens up for the two phases to flow parallel to each other. This is typically constructed by a circular tube, usually a small capillary, within a square or rectangular outer channel, where the dispersed phase flows in the capillary and the continuous phase flows in the outer channel [27]. It was first introduced by Cramer *et al.* [32], which inserted a micro-capillar into a rectangular flow cell.

Droplet Regimes for Co-flowing

Cramer *et al.* [32] present in a study that two distinct droplet breakup regimes exists for co-flowing devices: dripping and jetting. In the dripping regime the breakup occurs right at the tip, while in the jetting regime the droplets pinch off from a jet, i.e. an elongated thread of the dispersed phase. The dripping occurs at low flow rates for both fluids while jetting occurs at high flow rates, of either the dispersed or the continuous phase. These two regimes have also been confirmed by Utada *et al.* [31] which also states there are two dripping-to-jetting transitions; either a narrowing or widening jet is generated, see figure 2.5. In the dripping regime the growing droplets are subjected to two competing forces; viscous drag (pulling it downstream) and surface tension (holding it at the tip). When the drag force overcomes the surface tension droplet breakup occurs. Flow rate of the dispersed phase does not affect the droplet size in the dripping regime. Instead, the droplet size depend on the viscous drag that in turn depend on the flow rate of the continuous phase. However, if the flow rate of the dispersed phase increases, above a threshold, a widening jet is generated. If the flow rate of the continuous phase increases, above a threshold, a narrowing jet is generated. Droplet pinch off in the jetting regime is due to Rayleigh-Plateau instability [31].

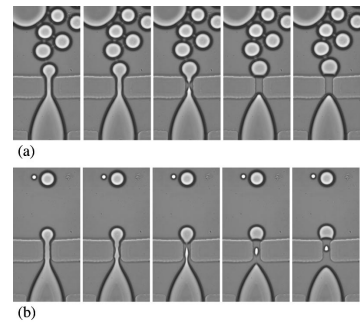

Figure 2.6: Experimental images of droplet breakup in a flow-focusing geometry. Droplet breakup occurs within the orifice, (a) uniform drops are generated; Q_c is 5.0 $\mu l/min$ and φ is 1/4, (b) small satellite droplets are generated with each large drop; Q_c is 25.2 $\mu l/min$ and φ is 1/40. Figure is from ref. [33].

Flow-focusing Devices

The final approach is to use flow-focusing geometries, which was first studied by Anna *et al.* [33] and Dreyfus *et al.* [34] where the dispersed phase is squeezed by two flows of the continuous phase. Anna *et al.* managed to form uniform droplets, where the breakup occurs within the orifice where the two phases are squeezed together.

Droplet regimes in Flow-focusing Devices

Four regimes can be found for flow-focusing geometries; squeezing, dripping, jetting and thread formation [27]. Due to the enormous possible geometrical aspects for this approach, there is no clear way to determine the transitions from one regime to another, nor for the droplet size and generation rate. However, the transition to the thread regime depends solely on the geometry and the flow field downstream in the channel [27].

2.2.3 Surfactants

Surfactants are often added to either the dispersed or the continuous phase and act to minimize the interfacial tension by stabilizing the interface between the two immiscible fluids. Surfactants are usually organic compounds of amphiphilic character; they posses both a hydrophobic and a hydrophilic part, see figure 2.7 a). Typically, surfactants are added to the continuous phase and can therefore facilitate the formation of new interfaces and to stabilize the formation of droplets or emulsions by ordering along the interface, see figure 2.7 b) [35]. The addition of such compounds will also stabilize the

droplets so the risk of coalescence of closely packed droplets or emulsions is minimized or eliminated [36].

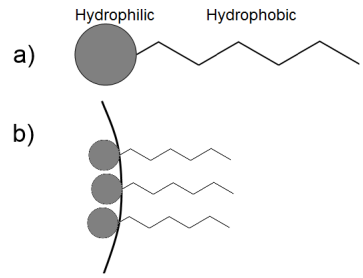

Figure 2.7: Schematic illustration of a amphilic surfactant (a) consiting of a hydrophilic (head) and a hydrophobic (tail), and order along an interface between two immiscible fluids (b) stabilizing the interface and lowering the interfacial tension.

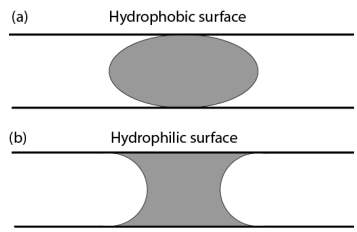

Figure 2.8: Schematic illustration of a water droplet (a) non-wetting a hydrophobic channel and a droplet (b) wetting a hydrophilic channel.

2.2.4 Hydrophobicity

One important parameter that must be set is the hydrophobicity of the channel walls in two-phase systems that utilize oil as the continuous phase, which is the case for water-in-oil droplet generation. As said before, a surface is said to be hydrophobic when the contact angle between a water droplet and substrate is above 90°, and hence, hydrophilic when the contact angle is below 90°, see figure 2.3. This is fundamental in two-phase systems since the droplets should not wet the channel walls, thereby allowing the droplets to flow continuously in the continuous phase. A droplet non-wetting and wetting a hydrophobic and hydrophilic channel, respectively, is schematically illustrated in figure 2.8. Usually the channels are treated with a solution that reacts with the channel surface and forms a self-assembled monolayer of molecules that have hydrophobic parts directed outwards from the surface, resulting in hydrophobic walls.

Chapter 3

Hypotheses

In addition to achieving a functional fabrication method for stable water-in-oil droplet generating systems and demonstrate flow regimes in T-junction and flow-focusing geometries, a few hypotheses were stated to be tested. Before going into the Materials & Methods, I will discus what I decided to test:

Flow Rates & Flow Rate Ratios

For a proposed and fabricated design of a droplet generating system the fluid flows and the relative flows, called flow rate ratio φ (defined as $\varphi = \frac{Q_{dispersed}}{Q_{continuous}}$), is assumed to affect the droplet size. With higher flow rate ratio an increased droplet size is anticipated, and vice versa. The impact of higher or lower flow rates for a constant flow rate ratio will be examined. This will be examined by doing experiments with flow rate constant for one phase while altering the other, as well as increase the total flow rate and keeping the ratio constant.

Surfactant Concentration

The addition of surfactant to the continuous phase could have an effect on the size or stability of the generated droplets. This will be examined by adding different amounts of surfactants to the continuous phase.

Channel Dimensions

By fabricating devices with different width at the droplet generating site the size of the droplets will alter. If the width is small, smaller droplets is anticipated to be formed compared to a wider width, for the same flow rates and flow ratios.

Chapter 4

Materials & Methods

4.1 Overview of the Methods

Both theoretical and practical methods are used to demonstrate droplet formation. The theoretical way is to simulate the droplet formation by using time-dependent computations in COMSOL Multiphysics®. This method is a complement to the practical method since the purpose of the thesis is to fabricate droplet generating systems and evaluate them. Thus, the practical method consists of fabricating devices and optimization of that method. Below are the two methods presented - a small part of the simulations and a more comprehensive part of the fabrication of different designs.

All detailed information of the equipments, fluids and chemicals used in the fabrication and experiments can be found in Appendix C.

4.2 Simulations

Simulations were conducted in COMSOL Multiphysics® to theoretically demonstrate droplet formation in two-phase microfluidics. The simulations were based on the Navier-Stokes equations for *laminar two-phase flow, level set (tpf)*. The two phases were set to water and Novec 7500, with the necessary fluidic properties (density and dynamic viscosity) presented in table 4.1. The simulations were performed both in 2D and in 3D - 3D-simulation yields neat visualization of the formed droplets and the interface of the two phases as well as the interaction of the dispersed phase to the walls. However, 3D-simulations are time-consuming (require several hours of computations), hence 2D-simulations were also conducted for its low computation time. The velocities for the two phases were often set arbitrarily, and were then altered to see the effect of different velocity ratios. Since the interfacial tension be-

tween Novec 7500 and water is not known to us, this parameter was set to 0.005 N/m (of the same magnitude to the value 0.0156 N/m that was used in [30]).

Table 4.1: Fluid properties of the two phases that were used in the simulations [37].

Fluid	Density (kg/m^3)	Dynamic Viscosity (mPa·s)
Water	1000	1.002
Novec 7500	1610	1.240

4.2.1 2D-Simulations

Two simulations were performed in 2D; one T-junction and one flow-focusing geometry. The geometry and dimensions are presented in figure 4.1. In the simulations the continuous phase was coloured blue and the dispersed phase red. The contact angle is set to $\pi/9$ [38].

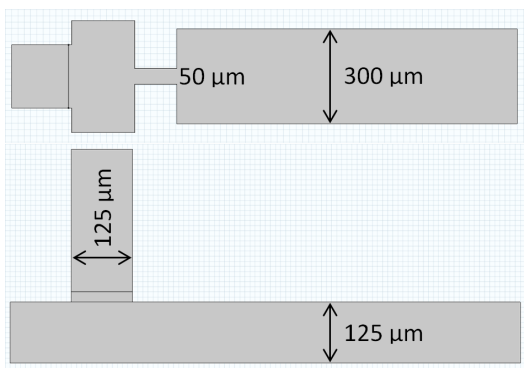

Figure 4.1: The two geometries used in the 2D simulations; flow focusing geometry (top) and T-junction (bottom).

4.2.2 3D-Simulations

One geometry was tested for 3D simulation: the T-junction. The geometry and dimensions are presented in figure 4.2. In the simulations the continuous phase was coloured blue and the dispersed phase red. The contact angle is set to $3\pi/4$.

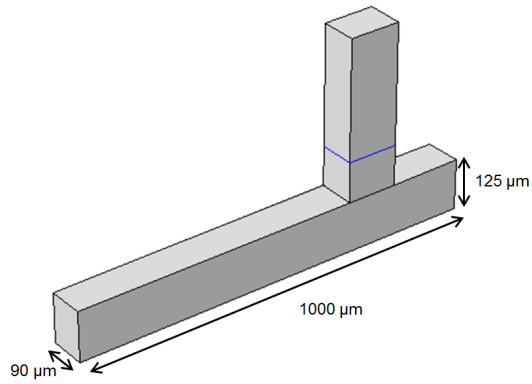

Figure 4.2: The model for 3D simulations; a T-junction with similar dimensions to the fabricated T-junction.

4.3 Fabrication

The experimental work consisted of fabrication and thereafter experiments on the fabricated devices. The method for fabricating the droplet generating systems was to use standard soft lithography, which will be discussed more in detail below. The method generally consists of fabricating a master by photolithography, that will be used to pattern an elastomer. The elastomer will then be detached from the mould and bonded to a substrate, usually a glass slide, and thereafter follows surface modifications. In this case, the channel walls will be modified to be hydrophobic.

4.3.1 Soft Lithography

Soft lithography is a non-photolithographic technique that are used in micro- and nanofabrication [9]. It consists of pattern replication from a mould, called master, which is created by photolithography - the transfer of a pattern to a photosensitive polymer commonly called photoresist, see figure 4.3 (a) - (d). The technique utilize a substrate, usually a silicon or glass wafer coated with a photoresist. The patterning is made when ultraviolet light are exposing the photoresist, but a photolithographic mask with precisely patterned opaque regions between the lamp and photoresist hinders the light from exposing all resist. The exposed polymer regions are chemically altered due to the ultraviolet light, and will be either soluble (positive photoresist) or cured (negative photoresist). After the exposure, the photoresist is developed in a solution called developer that chemically removes either exposed polymer (positive photoresist) or unexposed (negative photoresist) polymer. After this step the master is used in the soft lithography technique, where the

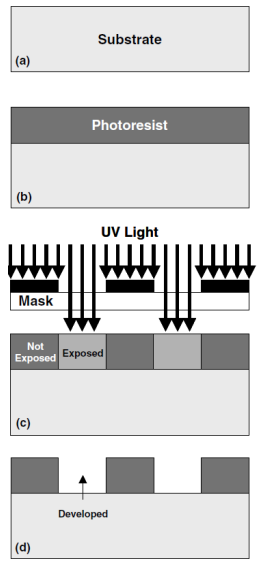

Figure 4.3: Typical process scheme for photolithography using a positive photoresist (a) - (d). Figure is cropped, from ref. [8].

patterned resist is used as a master for transferring the pattern to a polymer [39]. The polymer, usually an elastomer, is poured onto the master that after curing is formed to yield an inverse replica of the master. The formed elastomer is then detached from the mould and bonded to a substrate, usually a glass slide or another polymer. The process scheme of soft lithography used in this project is presented in figure 4.4. This technique offers advantages such as simple and a low cost process, high through-put and relatively rapid prototype developing period [39].

4.3.2 Device Fabrication

The water-in-oil droplet generation systems were fabricated by soft lithography, as described above, and the general process scheme can be seen in figure 4.4, but will be discussed in detail below.

4.3.3 Master Fabrication

The masters were made by photolithography where two different photoresists were tested; a photosensitive film called *SuperPHAT* and traditionally photoresist *AZ-125nXT-10A*. Both are of negative character, meaning, that the unexposed polymer will be removed during the development. The substrates on which the resists were applied on were 3" silicon wafers or 4" glass wafers.

The benefit of using the 3" silicon wafer is that they fit inside a petri dish that facilitates during PDMS moulding. If the master can be placed in a petri dish the PDMS can be poured into the dish without any PDMS spill. The benefit of using 4" glass wafer is that it is bigger and, hence, can hold more channel structures that can be fabricated simultaneously.

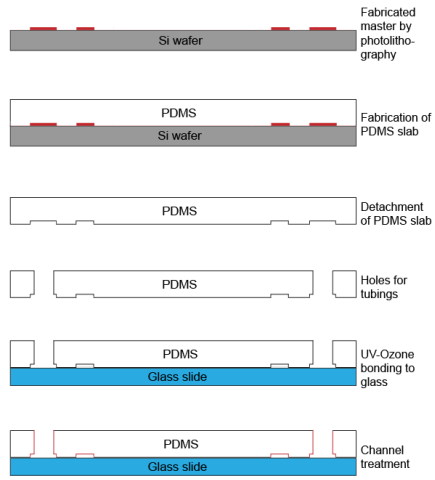

Figure 4.4: Process scheme of fabrication of devices for water-in-oil droplet generation by soft lithography; fabricate a PDMS slab, detachment it from the master, make holes for inlets and outlets, bond the slab to a glass slide, and lastly, make the channels hydrophobic.

SuperPHAT

SuperPHAT is a photosensitive film that was tested initially since it is a novel technique to be implemented in fabrication in the microscale but also because of the advantages of using a film; the film can be cut into desired pieces and attached to different substrates, and the thickness of the resist will always be the same. More advantages are that the spinning and baking steps are eliminated (which otherwise are required for traditionally photoresists). The development of the film is also a benefit compared to regular photoresists since only high pressurized water is used to develop the unexposed film and no chemicals are required. In addition, ultrasonic bath with short sonification pulses, can be used to remove the last remaining unexposed film. Tests with SuperPHAT films were performed with two different thicknesses: 400 μm and 100 μm, and were attached to 4" glass wafers using double-sided tape.

AZ-125nXT-10A

The AZ-resist was tested since that resist is intended for fabricating 100-120 μm high structure on substrates. That height was desirable since the channels were 125 - 300 μm wide and that would create more quadratic channels instead of rectangular channels with low height-to-width ratio. The resist was applied on substrates by spin-coating and both 3" silicon wafers and 4" glass wafers were tested as substrates. After the spin-coating follows a baking step before the UV-exposure. The protocol for fabricating the master using this resist can be read in Appendix D.1.

4.3.4 PDMS Moulding

When the master was fabricated an elastomer, polydimethylsiloxane (PDMS), was poured onto the master and let to cure. PDMS belongs to a group of polymeric organosilicon compounds, also called silicones, and is used because of its numerous advantages. PDMS is inexpensive, transparent (down to 230 nm), flexible, inert and non-toxic. At last, one big benefit of fabricating devices in silicone rubber compared to fabrication methods involving silicon or glass is that it with ease can be synthesized and bonded to other surfaces, [10]. The elastomer is also naturally hydrophobic due to its repeating $-OSi(CH_3)_2-$ units where the $-CH_3$ groups make it hydrophobic [10, 40], which is advantageous for water-in-oil droplet generation.

4.3.5 UV-ozone Bonding

A common technique to bond PDMS to glass is the UV-ozone bonding process [40]. Ultraviolet rays split oxygen molecules O_2 in the air into two separate oxygen atoms O that in turn reacts with an oxygen molecule O_2 to form ozone O_3. The formation and decomposition of oxygen molecules to ozone free oxygen atoms with high oxidizing ability can react with the surfaces of PDMS and glass. The $Si-CH_3$ groups on the PDMS chain are transformed into $Si-OH$ groups by the reactive oxygen atoms. The formed $Si-OH$ groups are then covalently bonded to the surface of the glass slide, yielding $O-Si-O$ bonds. This covalent bond yields a lasting and tight seal, with no leakage from the system. This technique is highly dependent on that both the PDMS slab and the glass slide is clean where no dust or other contaminants are present.

4.3.6 Channel Treatment

As mentioned in section 2.2.4, hydrophobic channel walls are essential for water-in-oil droplet microfluidics. Hydrophobic walls result in no wetting of dispersed phase to the walls, so the water droplets can flow continuously

inside the channels. The fabricated systems in PDMS and glass need to be coated with a solution to be hydrophobic. As said in the PDMS subsection, PDMS is naturally hydrophobic but can become hydrophilic during the UV-ozone treatment, and glass is naturally hydrophilic. The channel treatment was performed by inserting Repel-Silane, a solution consisting of dichlorodimethylsilane molecules, see figure 4.5, inside the channel by a syringe. The molecule binds to the surfaces inside the device and the methyl groups on the molecule will cause the channel walls to be hydrophobic. The solution was let to react with the surface of the walls, see figure 4.6 for the binding process of the silane to glass. Once the treatment is done the channels is immediately filled the continuous phase to make sure that only the continuous phase wets the walls.

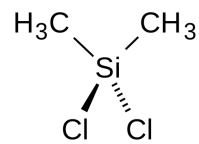

Figure 4.5: The dichlorodimethylsilane molecule, which is used in the fabrication. The methyl groups cause the surfaces to be hydrophobic.

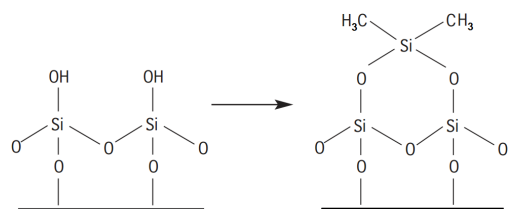

Figure 4.6: The binding of dichlorodimethylsilane to a glass surface; reacting with the hydroxyl group.

4.4 Designs

In the photolithography step a photolithographic mask is required, that has to be designed and fabricated before the photolithography starts. The chosen designs in this project were based on the flow-focusing approach and T-junctions. Based on the future intended application of combining droplets with acoustophoresis - focusing particles inside droplets or plugs - the channel widths were set to match the half wavelength for acoustic waves travelling through water. If the acoustic impedance of the channel walls are high enough

the width of the channel will result in a node for the arising standing wave inside the channel. However, the acoustic resonance of the elastomer used for the device is low, but were designed to combine with acoustophoresis anyway. To match the frequency of 6 MHz, which is one of the peak frequencies given by the piezoelectric transducer, and given that the speed of sound in water is roughly 1500 m/s the widths of the channel will be 125 μm, see Eq. 4.1.

$$Width = \frac{\lambda}{2} = \frac{1}{2} \cdot \frac{v}{f} = \frac{1}{2} \cdot \frac{1500\, m/s}{6 \cdot 10^6\, s^{-1}} = 125 \cdot 10^{-6}\, m \tag{4.1}$$

In addition to the channels that should be 125 μm wide, other channel designs were made with the varying width of 100-300 μm and were not intended to be combined with acoustophoresis. This width is utilized only for creating devices for drop generation, since to examine drop generation is the main purpose of this project. The varying widths are to make sure that differently sized droplets can be generated, e.g. so that 150 μm wide droplets can be generated. The photolithograpic mask was made by a mask writer at the department but required a drawing that the writer can comprehend and transmit to the wafer when writing the mask.

4.4.1 AutoCAD-drawing

The channels were designed and drawn in AutoCAD, see Appendix A.1. The designs in the mask are made with 125 μm wide main channels for $AI - AVI$ and varying 100-300 μm for $BI - BV$. Inspiration to designs AI, AII, AIV, DIII and DIV are from [41, 42]. $AI - IV$, $BIII$ and BIV are cross-junctions with a more narrow channel dimension at the junction site. AVI is a cross-junction without any narrowing dimensions, and AV and BV are T-junction where BV has a narrow inlet channel to the main channel. The smaller features at some of the junction sites are designed to see if it is easier to make small droplets compared to geometries without any small dimensions.

4.5 Optimization

After experiments on the fabricated devices a few optimizations were done, which resulted in a new photolithographic mask and an additional step in the fabrication method - silanization of the master.

In the new mask only drop generation was considered and is presented in Appendix A.2. The channel widths were widened, since this will lower the velocity of the formed droplets when they exit the orifice, and thereby enable the droplets to pass slower in the channel. The lower velocity of the fluid makes it possible for the camera to better resolve the droplets. Design CI

and CII are made with two different widths of the orifice to examine the significance of the dimensions, which is also done in DI and DII for the cross-junctions. Another design in the new mask was to connect the inlets for the continuous phase, which can be seen under the label *Reducing Inlets* in Appendix A.2. Also, a T-junction was drawn with smaller widths at the junction site to generate smaller droplets than was achieved in previous T-junction.

4.5.1 Silanization of Master

During the detachment of the PDMS slab from the master mould, residues from the elastomer were often seen. This results in non-perfect replicas of the master, and the design differs from the pattern on the AutoCAD drawing. To solve this problem a silanization modification of the master surface was neeeded. By silanizing the surface the detachment of the PDMS would be enhanced [10, 43]. The solution Repel-Silane was used again and was applied to the surface of the master. Repel-Silane is intended to prevent that polyacrylamide and agarose gels do not stick to glass surfaces [44], but was tested to see if a silanization could prevent PDMS residuals on the master.

Chapter 5

Results

In this chapter follows the results from the simulations, fabrication and results from the practical experiments. The first section presents the simulations, performed in COMSOL Multiphysics®, which was made to theoretically show droplet formation and also to see how the droplet formation changes when parameters such flow rates, flow rate ratios or interfacial tension are altered. The second section present the fabrication of a rigid and stable device without defects. The final section presents the results from the experiments where droplet regimes are examined as well as the three hypotheses, stated in the Hypotheses chapter.

5.1 Simulations

The simulations were made to theoretically demonstrate droplet formation in microfluidic systems. In the 2D simulation the flow rates and flow rate ratios were changed, which resulted in different sized droplets. In figure 5.1 four differently sized droplets are generated for four differently flow rates, while the flow rate ratio φ between continuous and dispersed phase is constant at 1/2. The diameter of the droplets decrease with increasing flow rates. In (A) and (C) a single droplet is formed while in (B) the main droplet is followed by a satellite droplet and in (D) a jet (or thread) is formed with a main droplet and a satellite droplet. In figure 5.2 a 2D simulation is presented that demonstrate the three different droplet regimes in T-junctions. By increasing the incoming flow rates, the capillary number is increased, and like figure 2.4 three regimes can be simulated. Both flow rates and flow rate ratios were altered to get the three regimes. The capillary number can be calculated since the interfacial tension is set to 0.005 N/m, and the velocities and viscosities are known. Also a 3D simulations is presented that demonstrates squeezing, dripping and jetting regimes, see figure 5.3. Also here the flow rates and flow rate ratios were altered to get the different regimes. Com-

mon for both T-junction simulations are that the different regimes appear at different capillary numbers and flow rate ratios.

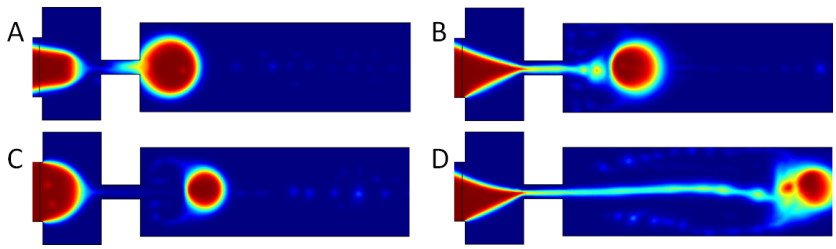

Figure 5.1: Simulations of droplet generation in a flow focusing geometry. Ca are (A) 0.003, (B) 0.005, (C) 0.015 and (D) 0.030, φ are 1/2 for (A)-(D).

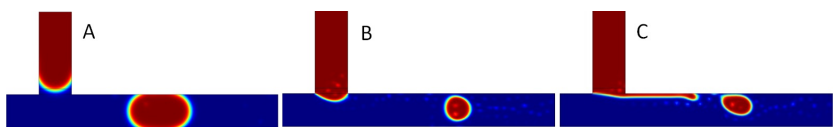

Figure 5.2: 2D simulations of droplet generation in a T-junction, where squeezing (A), dripping (B) and jetting (C) occurs. Ca is (A) 0.003, (B) 0.015 and (C) 0.020, φ is (A) 1/8, (B) 1/20 and (C) 1/14.

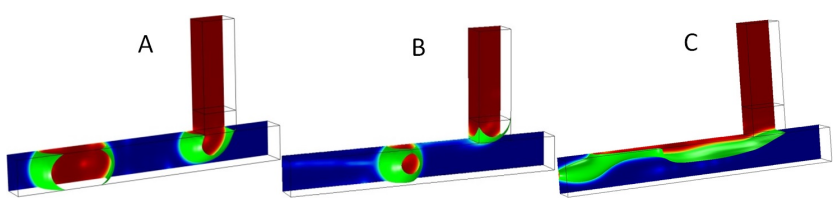

Figure 5.3: 3D simulations of droplet generation in a T-junction where squeezing (A), dripping (B) and parallel flows (C) occurs. Ca are (A) 0.003, (B) 0.02 and (C) 0.04; φ are (A) 5/6, (B) 1/12 and (C) 1/2.

5.2 Fabrication

Below follows the results from the fabrication during the project; most discussed are the two resists and the device fabrication.

5.2.1 Resists

The masters were made on 4" glass wafers and 3" silicon wafers. For practical matters the 3" silicon wafer was more convenient as substrate than the 4" glass wafer, because the silicon wafer could fit in a petri dish where the PDMS moulding occurred. The spinning time for the 4" glass wafer was slightly longer than for the silicon wafer to make sure that the whole wafer was covered with resist. No particular differences were seen after the development of the resist.

Two different resists were used to construct the master that later would be used to make a replica mould in PDMS - the photosensitive film SuperPHAT and the photoresist AZ-125nXT-10A.

SuperPHAT

Two different thick SuperPHAT films were tested - 400 μm and 100 μm. The exposure time, in the photolithography, was increased with every try-out since the cured film detached from the underlying substrate. The substrate on which the resist was attached was glass wafers. Pictures from the first try with SuperPHAT are given in figure 5.4; (A) with no ultra sonication and (B) with ultra sonication bath to remove more of the exposed polymer. The structures get more sharp definition and edges with sonication, but there are still remains of the resist near the glass wafer. About 10 seconds in the ultra sonication gave best results, at longer times the film detached from the substrate. Increased exposure time was tested to see if the adhesion to the substrate would be better and to see if more cured structures would be achieved. The pictures from the tests with longer exposure times are shown in figure 5.5; (A) with no ultra sonication and (B) with ultra sonication bath. The development of SuperPHAT resulted in some detachment of the film from the substrate. With longer exposure time the films were better attached to the substrate but could still fall off during the development. No fabrication experiments with SuperPHAT resulted in sharp and well-defined structures, however, longer exposure times and longer time in the ultrasonic bath gave sharper structures but, still, were not adequate as a master.

Since the SuperPHAT film did not results in any sufficient well-defined or stable structures, and the adhesion to the substrate was substandard no further fabrication was made with this resist. The SuperPHAT film may be good in easily making structures without chemicals but the small features required in microfluidics cannot be achieved in the film by using this method.

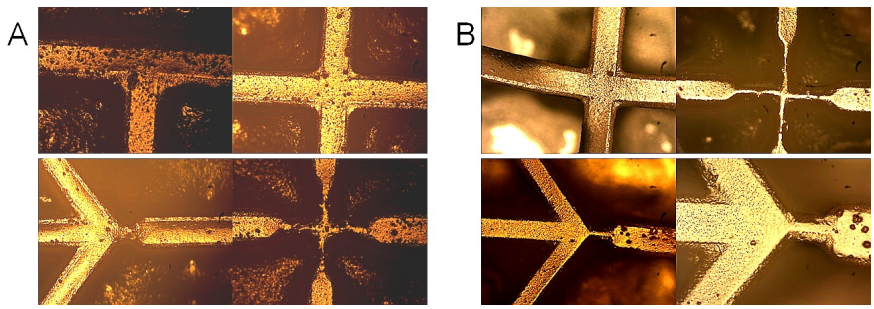

Figure 5.4: Pictures of some of the channels fabricated in 400 μm thick SuperPHAT. Exposure time: 200 sec, Development; ca. 2 min of pressurized water. (A) without sonication and (B) with sonication.

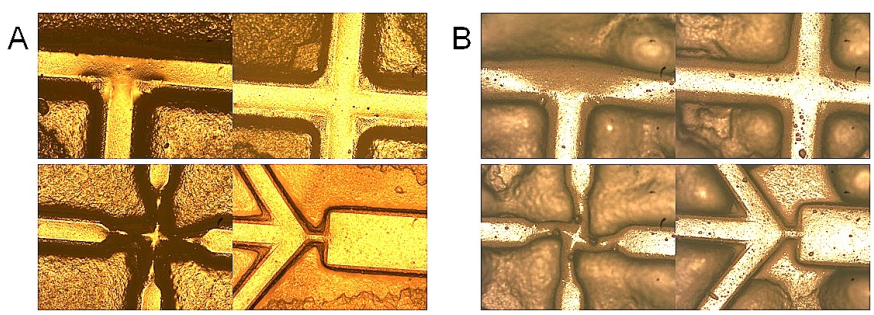

Figure 5.5: Pictures of some of the channels fabricated in 400 μm thick SuperPHAT. Exposure time: 300 sec, Development; ca. 2 min of pressurized water. (A) without sonication and (B) with sonication.

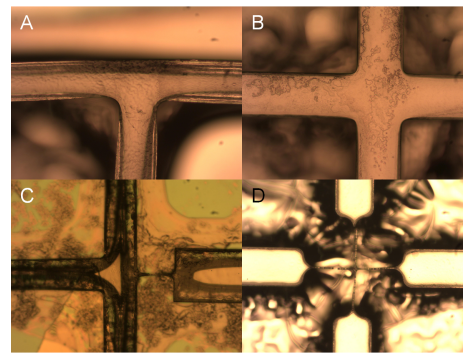

Figure 5.6: Pictures of some of the channels fabricated in AZ resist on silicon wafer. Exposure time: 60 sec. Large undercuts can be seen in (A), (C) and (D) that implies that the exposure time was not sufficient.

AZ-125nXT-10A

The second resist, AZ-125nXT-10A, was used to fabricate the master, and was spun on silicon wafers and on glass wafer. Many experiments were performed with the AZ resist before an optimized process scheme gave sufficiently good masters. The spinning velocities were taken from the distributor guidelines [45] and the exposure time in photolithography was set to 60 seconds. The development of the exposed resist consisted of repetitive development in AZ 326 Developer and rinsing in MilliQ-water. It was obvious that the exposure time of 60 seconds was not sufficient. Some of the structures were completely removed from the substrate and those that remained showed sign of undercuts, see figure 5.6. The exposure time was increased to 2 minutes but still resulted in structures with undercuts but all exposed resist remained on the substrate. The exposure time was increased to 5 minutes and resulted in structures with low undercuts, see figure 5.7. However, the small features had relatively big undercuts. At the exposure time of 7 minutes the undercuts were almost eliminated and the small features remained without undercuts, see figure 5.8, where also the widths are presented. The widths of the structured resist are smaller than the drawn widths; for the main channel the reduction of width was approx. 1 %, but for the small features in (D) and (E) the reduction was 6 and 10 % and for (F) it was 28 %. The measured heights were in average 85 μm.

5.2.2 Device Fabrication

When the master was fabricated the soft lithography process started. After the PDMS had cured it was diced and holes for tubings were made, then bonded to a glass slide and rubber tubings glued to the inlets and outlets,

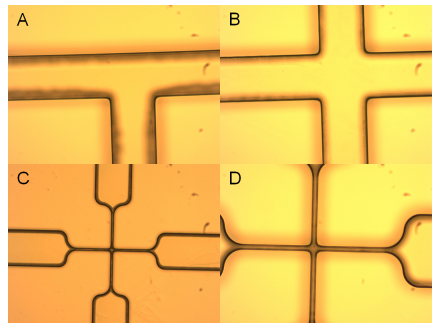

Figure 5.7: Pictures of some of the channels fabricated in AZ resist on silicon wafer. Exposure time: 5 minutes. Small undercuts can be seen in (A) - (D) that implies that the exposure time was still not sufficient.

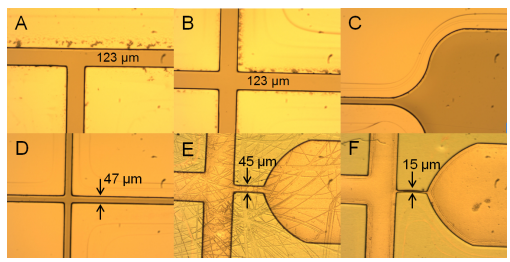

Figure 5.8: Pictures of some of the channels fabricated in AZ resist on silicon wafer, including measured widths. Exposure time: 7 minutes. Devices from design: (A) AV, (B) AVI, (C)-(D) DI, (E) CI and (F) CII.

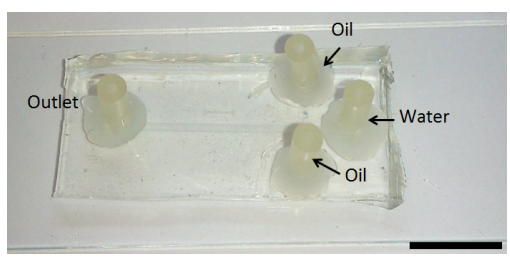

Figure 5.9: Picture of a fabricated device. Inlets for the continuous (oil) and dispersed (water) phases and outlet are given. Scale bar is 1 cm.

see figure 5.9. The first fabricated devices were defect due to PDMS residuals that remained on the master. Example pictures of defect devices, can be seen in appendix B. The silanization of master was introduced in the fabrication process that solved the problems with PDMS residues. Pictures of fabricated devices that were successful in the detachment can be seen in the figures 5.10, 5.11, 5.13, 5.16, 5.15 and 5.18.

5.3 Droplet Generation

As in other microfluidic systems the Reynolds number is low for the fabricated devices, and one can assume laminar flow. A quick calculation of the dimensionless number, using Eq. 2.3, indicate this:

$$Re = \frac{\rho D_H v}{\mu} = \frac{1610 \cdot \frac{4(90 \cdot 200)10^{-6}}{(2 \cdot 90 + 2 \cdot 200)} \cdot 0.02}{1.24 \cdot 10^{-3}} \approx 2.96 \tag{5.1}$$

Where the channel is assumed to be completely filled with the continuous phase, channel cross-sectional area is 90·200 μm^2, the velocity is 0.02 m/s (calculated by the flow 20 μl/min), ρ is 1610 kg/m^3 and μ is 1.24 mPa·s (see table 4.1). Reynolds number is approx. 2.96 for this case, and will not increase significantly for wider channels or increased flow rates. At this low Reynolds number viscous effects and forces dominates over inertia. In addition, laminar flow (or streamline flow) occurs since the Reynolds number is much less than 1500. Also the Weber and Bond number are low (< 1), why the inertial effects can be neglected in our experiments. (Since the interfacial tension between the two phases is not known We and Bo are calculated by using an surface tension of 0.005 N/m as used in the simulations.)

The fabricated droplet generating systems were made by master fabricated in the AZ resist. The first fabricated devices where done without the optimized fabrication method, and resulted in defect devices since PDMS residues remained on the master during the detachment. The droplet generation was observed in some of these defect devices but because of their non-perfect structure the hypotheses were not tested on these. Figures of these fabricated devices can be seen in Appendix B, which also shows that droplet generation works in these systems as well, but cannot give reliable results for the experiments. Often were polydisperse droplets generated and no stable generation achieved.

After the optimization step in the fabrication process the PDMS detached from the master without leaving any residues and the device could be used to test the hypotheses.

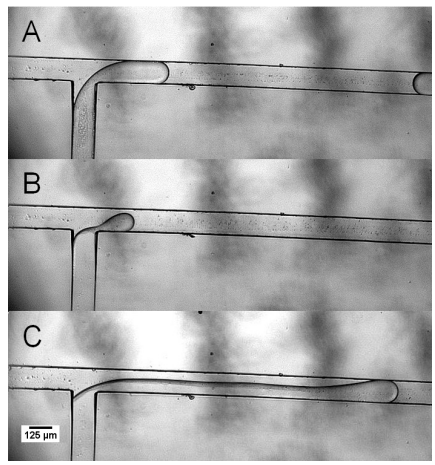

Figure 5.10: Transition from squeezing (A), dripping (B) and jetting (C) in a fabricated T-junction. Flow rates Q_d are (A) 1, (B) 5 and (C) 10 μl/min; flow rate ratios φ are (A) 1/4, (B) 1/4 and (C) 1. Scale bar is 125 μm.

A fabricated T-junction was used to prove the three different droplet regimes for that approach: squeezing, dripping and jetting. As said in the Droplet Formation chapter the three regimes exist at different capillary numbers. In figure 5.10 the three different regimes can be seen, where the squeezing regime generates plugs in the channels, the dripping regime generates droplets that are in the same size as the channel or smaller. The last regime, jetting, can be seen by the characteristic jet that forms at the water inlet. In this experiment 2 % v/v of surfactants was are used in the continuous phase. The interfacial tension between Novec 7500 (continuous phase) and MilliQ-water (dispersed phase) are not known, and could not be found in literature. The capillary number at the different regimes can therefore not be calculated for these experiments. Another fabricated device was a cross-junction, which is a flow-focusing geometry since the dispersed phase is squeezed between two flows of the continuous phase, and also here the different regimes could be found. As stated in the Droplet Formation chapter it is hard to see the transition from squeezing to dripping for flow-focusing devices due to the enormous possible geometries. However different droplet breakups can be seen in the cross-junction. The droplet breakup can occur at the cross-junction or downstream of the cross-junction. Additionally, the three incoming flows can flow parallel in three streams downstream without pinching. These droplet breakups were achieved in the fabricated cross-junction at different flow rate ratios φ and capillary number, see figure 5.11. In this experiment 2 % v/v of surfactants was used in the continuous phase.

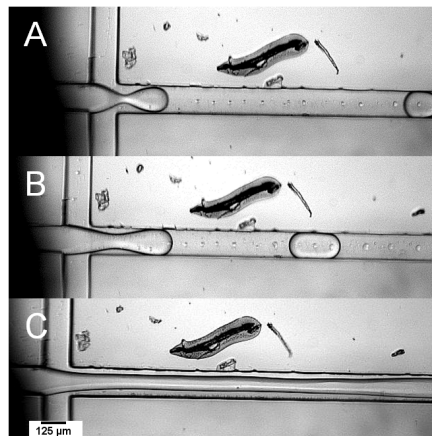

Figure 5.11: Transition from droplet break up at cross-junction (A), downstream of the cross-junction (B) and parallel flows (C). Flow rates Q_d are (A) 10, (B) 1 and (C) 50 μl/min; flow rate ratios φ are (A) 1/4, (B) 1/2 and (C) 5/2. Scale bar is 125 μm.

5.3.1 Flow Rates & Ratios

One of the hypotheses given in the Hypotheses chapter was that a decreased flow rate ratio φ will result in smaller droplets. That hypothesis was tested in many devices, where two results are presented in figures 5.12 and 5.14. One of the tested devices were based on the *DIV* design and the other was based on *CI*. For *DIV* a constant flow rate of the dispersed phase of 1 μl/min was used, while for the *CI* three constant flow rates of the dispersed phase 2, 4 and 6 μl/min were used. The flow rate of the continuous phase was altered during the tests. It clearly shows that a decreasing flow rate ratio results in smaller droplets and that an increased total flow in the system lowers the droplet diameter, see figure 5.14. This due to the increased shear rate at higher flow rates of the continuous phase. The increased total flow also increases the capillary number in the system, which is why the droplet diameter decreases with higher total flows.

5.3.2 Surfactant

The second hypothesis was the surfactant dependency; if a variation of concentrations of the added surfactant (Krytox) would give differently sized droplets. This was tested in a device based on the *CI* design, because it was one of the most stable droplet generating designs and the wide main channel makes it easy to resolve the generated droplets. The different concentrations were 0 %, 1 %, 2 % and 4 % v/v of surfactant dissolved in the

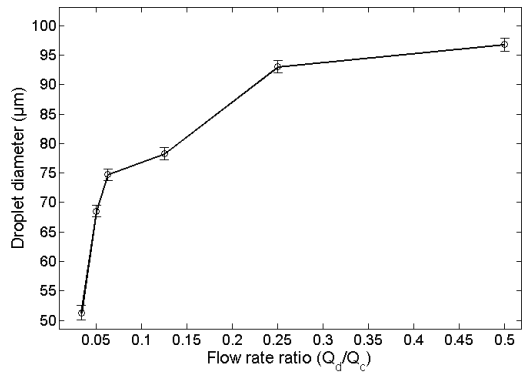

Figure 5.12: Graph showing droplet diameter as function of the flow rate ratio. Dispersed phase flow rate is contant at 1 $\mu l/min$. Plotted are mean ±SEM (Standard Error of the Mean), mean dispersity is 1.3%

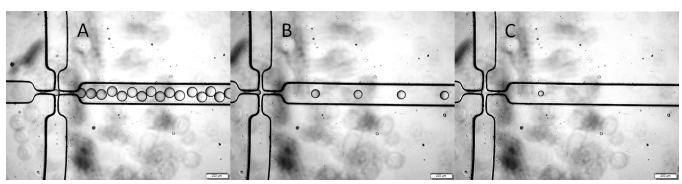

Figure 5.13: One of the fabricated devices, from design DIV, in which the flow rate ratio hypothesis was tested. Q_d is constant at 1 μl/min; flow rate ratios φ are (A) 1/2, (B) 1/16 and (C) 1/30. Scale bar is 200 μm

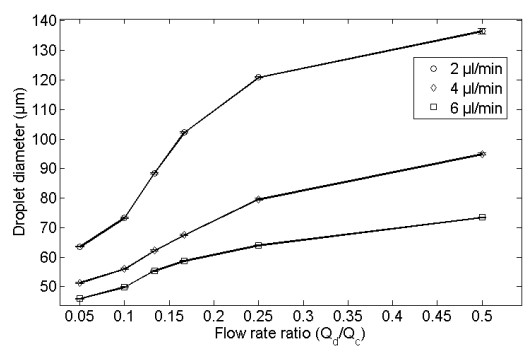

Figure 5.14: Graph showing the droplet diameter as function of flow rates and of flow rate ratios (φ). Dispersed phase flow rates are 2, 4 and 6 μl/min. Plotted are means ±SEM (Standard Error of the Mean), dispersity range from $1.0 - 2.6\%$

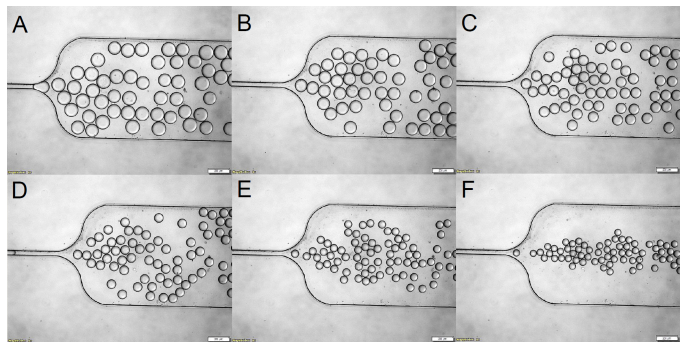

Figure 5.15: One of the fabricated devices, from design CI, in which the flow rate ratio hypothesis was tested. It can be seen that the generated droplets get smaller diameter when the flow rate ratio decreases. Q_d is constant at 2 μl/min; flow rate ratios φ are 2/4 (A), 2/6 (B), 2/8 (C), 2/10 (D), 2/15 (E) and 2/20 (F). Scale bar is 200 μm.

continuous phase. The test with 0 % surfactant resulted in very unstable droplets, where coalescence occurred directly when two droplets or plugs encountered each other. That experiment can be seen in figure 5.16, where big plugs or blocks of the dispersed phase fill up the channel. The blocks are hard to move since the continuous phase does not affect or interact with the dispersed phase. For the experiment when 1 % Krytox was used only a small risk of coalescence occurred, while no coalescence where seen when 2 % and 4 % surfactant concentrations were used. The experiments shows that an increased addition of surfactants decreases the droplet diameter, see figure 5.17. The flow rates for the two phases were the same for every test, only the surfactant concentrations in the continuous phase were changed.

5.3.3 Channel Dimension

The channel dimensions play a huge role in droplet generation. The dimensions and geometries give rise to flow fields for the two phases in the system and as stated in the Droplet Formation section, the flow fields deform the interface and induce instabilities that promote droplet breakup. An example can be seen in a flow-focusing device with two different width of the orifices, 41.9 μm and 11.3 μm, see figure 5.18. The flow rate of the two phases are same in both tests but due to the very small orifice in (B) much smaller droplets are generated than in (A). The generated droplets in (B) are in mean 23.5 μm in diameter, which is approx. 7 picoliter while the mean diameter for the droplets in (A) is 70.6 μm, which is approx. 180 picoliter.

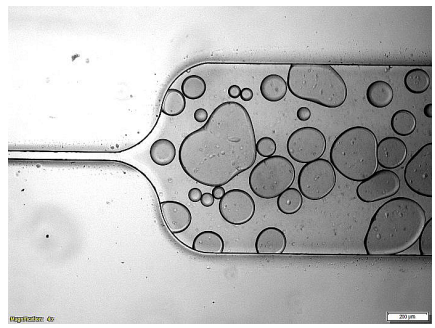

Figure 5.16: Figure showing an experiment where no surfactant was added to the continuous phase. Coalenscence occured directly when two droplets encountered each other, which results in big plugs or blockages of the dispersed phase inside the channel. Scale bar is 200 μm.

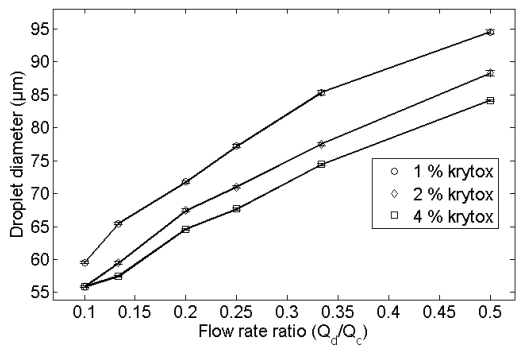

Figure 5.17: Graph showning the depency of the addition of Krytox. 1 %, 2 % and 4 % v/v Krytox concentrations are used in the experiments. Dispersed phase flow rate is contant at 2 $\mu l/min$. It can be seen that smaller droplets are generated with higher concentrations of the surfactant. Plotted are means ±SEM (Standard Error of the Mean), dispersity range from $0.8 - 1.4$ %.

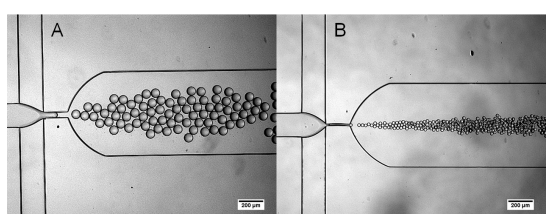

Figure 5.18: Two devices with different widths of the orifice generate differently sized droplets for the same flow rates of the two phases. The volume of the droplets in (A) are approx. 180 picoliter while the droplets in (B) are approx. 7 picoliter. Q_d is 2 μl/min, flow rate ratio φ is 1/10. Scale bar is 200 μm.

Chapter 6

Discussion

6.1 Simulations

In the simulations some assumptions were made. The interfacial tension was set to 0.005 N/m, because this value is in the same magnitude for the simulations in [30], and also because this value worked well for the simulations. The contact angles were not the same for the 2D and 3D simulations, this due to the fact that in the 2D simulations the angle concerned the continuous phase and in the 3D simulations it concerned the dispersed phase. Meaning, the continuous phase should wet the channel wall, therefore should the contact angle be less than $\pi/2$ and the dispersed phase should not wet, thus, should the contact angle be bigger than $\pi/2$. Next, the fluid velocities were chosen arbitrarily and were not based on the experimental work.

The simulations have shown that it is possible to theoretically demonstrate droplet formation in microfluidic systems. Simulations are a very convenient way to test new designs or approaches before the practical work is done, as long as all fluidic and other properties are known. The results from the performed simulations have shown the formation of differently sized droplets at varying flow rates and also demonstration of droplet regimes for different capillary numbers and flow rate ratios in a T-junction. 2D simulations as well as 3D simulations have shown to give qualitative simulations but 2D is to prefer since the calculation time (several minutes for 2D and several hours for 3D) is dramatically decreased compared to 3D. A problem with the 2D simulations was the thickness of the interface between the two phases. To get a neat and good simulation of droplet formation a thin interface is desired, but that requires a very detailed mesh. With a highly detailed mesh the number of calculations are increased and thus the computation time is increased. Therefore, a balance between interface thickness to the computation time has to be considered.

6.2 Experimental Work

The fabrication method resulted in fully functional droplet generating systems, where a moulded PDMS slab was bonded to a glass wafer. After hydrophobic surface modification of the channel walls there was low or eliminated wetting of the dispersed phase to the walls, which is essential for water-in-oil droplet generation. Evidence of wetting can be seen in figure 5.11 where extremely small water droplets have attached to the glass wafer. Fortunately this did not affect the droplet generation in this device. PDMS is by itself hydrophobic but glass is hydrophilic why it is essential that the surface modification works. The PDMS moulding was only done on masters fabricated in the AZ resist since the photosensitive film SuperPHAT did not result in any satisfactory masters. Both 100 and 400 μm thick films were tested, were non gave good result. The AZ resist resulted in well reproduced masters compared to the dimensions from the photolithographic mask. The wide parts only differed a few % compared to the dimensions in the mask, but, for the 20 and 50 μm features higher differences were seen (10 - 28 %). This is problematic, especially if those small features are required in the device. The solution could be to further increase the exposure time, thereby allowing more UV-light to expose the resist.

Before the fabrication process was optimized with silanization the detachment of PDMS from the master was problematic. Almost every time there were PDMS residues remaining on the master. This does not only result in defect devices but also ruins the master for any further PDMS moulding. The silanization of the masters simplified the detachment of PDMS slabs and no residues of the elastomer were seen on the master. However, one problem with the silanization process is that one does not know if a monolayer of the silane has completely covered the surface. Any remaining solution left had to be wiped off with a soft tissue. The wiping with tissues may harm the master and/or introduce contaminations to the PDMS. A better method for the silanization process would be beneficial. Additionally, contaminations can also be introduced in the UV-ozone bonding process, why it is important to keep the surfaces of the glass wafer and PDMS slab as clean as possible. Dust that has stuck in the PDMS and between the PDMS and glass can be seen in figure 5.11. This may prevent a tight seal; that can cause leakage or even detachment pf the PDMS slab from the glass wafer. Therefore, is it preferable to work as much as possible in clean room environment, where the risk of introducing dust or other contaminations is reduced.

As just mentioned, the fabricated devices are, as most devices in the nano- and microscale, very sensitive to contaminations. These were often intro-

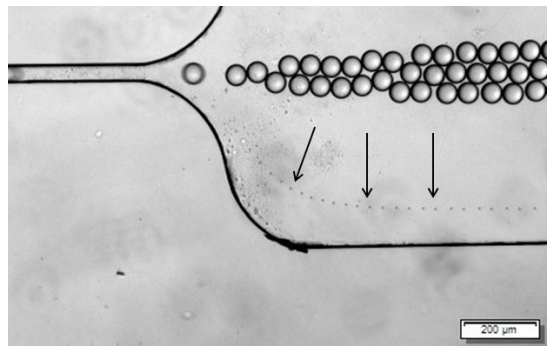

Figure 6.1: The phenomenon of satellite formation in addition to the main droplet are seen for some flow rates and flow rate ratios. Satellite droplets are seen as very small dots below the larger droplets. Scale bar is 200 μm.

duced during the experiments, and could in worst case ruin the whole device. If dust entered the device it eventually would get stuck in the small features for some devices. Often it could be solved, by using hand, to drag the fluid out from the inlet and hopefully would the dust follow the fluid. To limit contaminations cellulose filters were placed at the syringes, which successfully lowered the risk of dust entering the systems. However, the risk of introducing contaminations when tubings were inserted or removed from the inlets and outlets still remained.

A well known and often observed phenomenon in droplet microfluidics is the production of satellite droplets, or secondary droplets, that form in addition to the main droplet, see figure 2.6. The formation of satellite droplet is due to recoil movements when the larger main droplet separates from the dispersed phase. This phenomenon is often unwanted, since a precise and monodisperse droplet generation is often desired. Satellite droplets have been seen in the systems tested in this project; at some flow rate ratios they are present while at another ratio are they not formed, see figure 6.1. The satellite droplets have shown not to be present at low flow rates for the continuous phase, e.g. in the squeezing regime for T-junction. But are present when the flow rates of the continuous phase are high, implying that the formation of satellite droplets are due to the capillary number in the system.

The first presented results from the droplet generation proved the different droplet regimes in T-junctions by changing the flow rates and flow rate ratios. Similar results are presented in a study by Liu and Zhang [30], which by numerical simulations showed the regimes in a T-junction for different capillary numbers and flow rate ratios. Next, the droplet formation in a cross-junction

where found to occur at the cross-junction, downstream of the cross-junction and eventually stable parallel flows were formed. The transitions depends on both the flow rates and the flow rate ratios of the incoming fluids. These flow patterns are also presented in another study by Liu and Zhang [46] by numerical simulations. They present that the flow regimes are dependent on the capillary number and flow rate ratios of the continuous and dispersed phases.

In chapter 3 there were three hypotheses stated, which were tested during the experimental work and will be discussed below.

By altering the flow rate ratios the generated droplets' sizes were changed, which can be seen in figures 5.12 and 5.14, which proves the hypothesis that lower flow rate ratio decreases the sizes. This is also presented in other studies; where the flow rate of one phase is constant while varying the other phase, which results in a range of droplet diameters [36, 47, 48]. In addition, by changing the total flow rates while keeping the ratio constant, smaller or bigger droplets were formed, see figure 5.14. This is also observed in the simulations , see figure 5.1. Since the formation and breakup of a dispersed phase into droplets or plugs is a balance between interfacial tension, holding the interface intact, and the shear rate, tending to deform the interface, higher flow rates of the continuous phase will increase the shear rate and hence droplets with smaller diameter are formed.

Further, the experiment with different concentrations of surfactant added in the continuous phase implies that the addition of surfactant will not only stabilize the droplets but also lower the interfacial tension between the two phases. As seen in figure 5.17 the generated droplets' diameter decreases with higher surfactant concentration. This phenomenon is explained by the fact that the addition of surfactants tend to lower the interfacial tension between the two phases that in turn increases the capillary number for the system. Hence, smaller droplets are generated. Similar experiments were performed by J. Tan *et al.*, where they examined the effect of different surfactant (Span 80) concentrations added to a continuous phase (anhydrous octane) by measuring the length of dispersed plugs (deionized water) in a cross-junction [48]. They found that the plug length was independent of surfactant concentration because the interfacial tension reaches minimum value for their lowest tested surfactant concentration, which was more than critical micelle concentration (C_{mc}). (C_{mc} is generally defined as the surfactant concentration above which micelles form). Meaning, that before reaching C_{mc} the interfacial tension changes highly with small additions of surfactant, and will eventually level off to a lowest value [49]. Further, the results presented in this thesis may depend on that the C_{mc} was not reached and the interfacial tension was

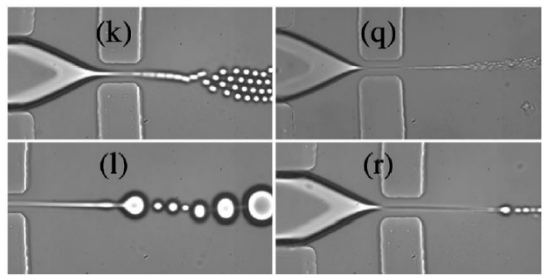

Figure 6.2: Jetting regime in a flow-focusing device. Due to high flow rates and low flow rate ratios are droplets with smaller diameter than the orifice width generated. Q_c are (k) and (q) 252 μl/min, (l) and (r) 498 μl/min; φ are (k) and (l) 1/40, (q) and (r) 1/400. Figure is cropped from original figure in ref. [33].

changed for all three surfactant concentrations. The C_{mc} for this continuous phase and surfactant are not known nor found in the experiments. The test of different channel dimensions in this project show that for the same flow rates and flow rate ratios differently sized droplets are generated depending on the width of the orifice, see figure 5.18. This is explained by the increased fluid flow in the smaller design, which in turn increases the shear stresses acting on the dispersed phase. The formed droplets tend to have a smallest diameter comparable to the width of the orifice they exit from. To generate smaller droplets high flow rates of the continuous phase with very low flow rate ratios are required, see figure 6.2. Such approach is not often desirable since it consumes large quantities of fluid, and therefore is it convenient to design systems with orifice widths in the size of the aimed droplet diameter. However, the small width of the orifice cause the resistance to increase. Especially for the designs tested, see figure 5.18, the resistance was so high that the incoming fluids were hard to get through the orifice. Instead the fluids would flow to one of the three inlets that caused the tube in that inlets to be pushed out of the rubber tubing and the experiment had to start over.

Many of the drawn designs in the first photolithographic mask are not presented as devices in this thesis. This is due to that many of the fabricated devices became defect during the detachment of the PDMS, and were not used to test the stated hypotheses. Some of those designs were not fabricated again after the optimization step. Instead, the designs drawn in the second mask and the *DIV* design were used to test the hypotheses. This because these geometries lowers the velocity (due to the wider channel) so droplets can be resolved easier by the camera. The designs *AV* and *AVI* were used to see the different droplet regimes in T-junction and cross-junction.

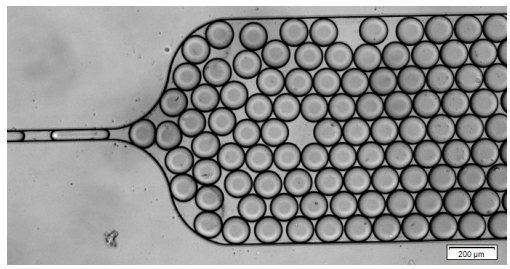

Figure 6.3: Monodisperse droplet generation is achieved, where the dropelts can form dense packing. Q_d is 1 μl/min and φ is 2. Scale bar is 200 μm.

Experiments have also shown that a common inlet for the continuous phase, see *Reducing Inlets* in Appendix A.2, works just as well as using separate inlets. However, there can be problems if contaminations are in one of the channels. This will cause higher resistance in that channel and the fluid will not flow evenly divided in the two channels.

The graphs presented in figures 5.12, 5.14 and 5.17 plots the mean and SEM. However, the SEM are not always visible since the values are very small. These small values results in low dispersity (ranging approx. 1-3 %), which indicates that monodisperse droplets are generated in the systems. Another evidence that monodisperse droplets have been formed is the ability for dense packing, which can be seen in figure 6.3. If polydisperse droplets would be generated this kind of packing would not occur.

Chapter 7

Conclusion

The simulations performed have shown droplet formation in a T-junction and flow-focusing geometry. The results from the simulations prove that droplet size and droplet regimes depends on the capillary number in the system and on the flow rate ratios of the two phases. Squeezing, dripping and jetting regime is found by simulation in 2D T-junction by altering the velocities, i.e. changing the capillary number, and flow rate ratios of the incoming fluids. 2D simulations can be used to numerically do fast droplet formation analysis while 3D simulations require more time and computer power but results in neat visualizations of the interface between the two phases.

The experimental work has shown that the photosensitive film SuperPHAT is not sufficient for fabricating masters for PDMS moulding without further optimization. The small features required in these devices are not achievable and the attachment of SuperPHAT on the substrate was insufficient. No droplet generating devices were fabricated by SuperPHAT masters. The AZ resist resulted, after optimization of exposure time, in satisfactory masters which were rigid with sharp edges, firmly attached to the substrate and stable for multiple PDMS moulding. The soft lithography process was optimized with a silanization of the masters so that the detachment of PDMS did not leave any residues and the masters could be used for further moulding. The UV-ozone bonding resulted in well sealed devices with long lasting bonding, and the channel surface modification showed little or no wetting of the dispersed phase to the walls.

The results from the experimental work have shown devices that generate monodisperse droplets and that the droplet size depends on the channel dimensions, flow rates, flow rate ratios and surfactant addition. Small channel dimension result in increased shear rate, which is responsible for the droplet breakup, and hence smaller droplets are formed in those systems compared

to larger channel dimensions for the same flow rates. Increased flow rate increase the capillary number in the system that result in smaller droplets, which is also seen for decreasing fluid flow ratios. The addition of surfactant to the continuous phase have shown to stabilize the droplets and coalescence is eliminated or very rare. Different surfactant concentrations in the continuous phase are shown to lower interfacial tension and smaller droplets are formed with higher concentrations.

7.1 Future Improvements

For future work in the droplet microfluidics field, a few improvements are suggested. In the fabrication process could SU-8 be used instead of the AZ resist. SU-8 is also a negative photoresist and it is frequently used for fabricating masters by soft lithography [36, 41, 50, 51]. Different forms of SU-8 are available for fabricating structures of different heights, and yields a very stable structure attached to the substrate. Another improvement is to use smaller tubings, since they can be inserted into the holes in the PDMS slab, meaning that no gluing of rubber tubings are required. Tubes can also be placed at the inlets and outlets on the master before pouring on PDMS and during the curing the tubes are automatically attached in the device, thus, no holes for tubings are required at all. Further, instead of bonding the PDMS slab on a glass slide, the bonding substrate can be another smooth PDMS slab (without any channels). Since PDMS is naturally hydrophobic the surface modification can be eliminated. In this project Repel-Silane was used for the channel surface modification and worked adequately, however, another solution called Aquapel could be used instead. The surfactant used in this project (Krytox) is a poly(perfluoropropylene glycol)-carboxylates [36] but another surfactant could be used instead, e.g. the EA surfactant (sold by RainDance Technologies), which is a polyethyleneglycol (PEG) coupled to perfluorinated polyethers (PFPE). The Krytox surfactant has charged headgroups that can interact with other charged molecules, such as DNA, RNA and proteins. The interaction can unfold the biomolecules' higher-order structure at the drop interface, which is unwanted in biological assays, and hence the EA surfactant could be used. That surfactant is biocompatible and efficient in stabilizing emulsions [36].

Another approach is to fabricate the two-phase systems in glass isotropically etched by HF and bonded to another etched glass wafer for a more rigid device with circular channels. Although, in such systems surface modification are essential and important for achieving hydrophobic walls.

Chapter 8

Popular Scientific Summary

The field of microfluidics is a research field that manipulates very small volumes of fluids, most often liquids. As the name implies, this is performed in the microscale where *micro* is a prefix for a millionth part. The devices for microfluidics have channels that are in sizes of a few to hundreds of micrometers (million part of a meter). Microfluidics emerged in the beginning of the 1980s, for development and applications in inkjet printers, but later applications for other fields, such as physics, chemistry, biochemistry, nanotechnology and biotechnology emerged.

One subfield of microfluidics is droplet microfluidics, which manipulates dispersed droplets, or packages, of one fluid encapsulated inside another continuous fluid. The two fluids have to be immiscible, meaning that they will not form a homogeneous mixture and a distinct interface will form between the fluids. This is comparable with water droplets in oil, the two liquids will not form a homogeneous mix but a visible boundary will form between them. In droplet microfluidics these droplets have volumes ranging from microliters down to picoliters and the droplets can be used in assays for biological or

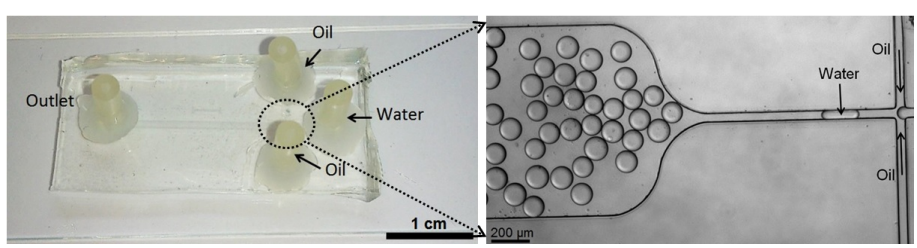

Figure 8.1: A microfluidic device (left) fabricated in this MSc work for droplet generation. 4x magnified picture of the cross-jucntion (right) of a fabricated device, showing the incoming oil and water.

chemical experiments. Example, if two or more solutions are to be mixed or cells are to be analysed in a specific solution, they can be fused into droplets and due to the small volumes full mixing occurs fast and analysis of the assays can be done immediately.

The major advantages of using droplets or small packages of one fluid encapsulated inside another are that each droplet work as isolated reactors and that each droplet can be analysed separately, which opens up for serial and parallel reactions. These advantages increase the through-put compared to traditionally assays but also lowers the waste, lowers costs (due to small volumes of solutions required) and lowers the risk of handling errors. Droplet microfluidics has therefore a big potential for medical research, diagnostics, single cells analysis, gene therapy, polymer emulsions and many more.

In a MSc Thesis work at the Faculty of Engineering, LTH, at Lund University, have droplet generating devices been fabricated, to examine how a few parameters affect the droplet formation. One fabricated device for generating droplets can be seen in figure 8.1, where a silicone rubber (PDMS) has been moulded and bonded to a glass slide. The rubber is moulded after a stamp, called a *master*, which yields an inverse replica when detached from the master that results in channels when bonded to a glass slide. Two approaches for achieving droplets were tested - T-junction and flow-focusing geometries. In both approaches is a dispersed fluid injected into a continuous fluid. In the experiments water was used as the dispersed fluid and an oil, an hydrofluoroether (HFE), as the continuous fluid. For water-in-oil droplets, the oil has to wet the channel walls thus the surface of the walls has to be modified to be hydrophobic. To stabilize the droplets (so that they do not coalesce with each other) surfactants are added to the oil. A surfactant is a compound that arranges along the interface between the two immiscible fluids and stabilizes the droplets but also lowers the surface tension between the two fluids.

In the experiments were different flow rates and flow rate ratios of the two fluids tested, as well as different surfactant concentrations and how the channel dimensions affect the size of the droplets. The device is positioned under a microscope with a mounted camera where the droplet generation can be observed and recorded. The fluids are injected into the device by syringes driven by syringe pumps. Generation of water-in-oil droplets can be seen in figure 8.2, where monodisperse droplets of approx. 0.9 nanoliters are continuously generated.

The experiments showed that the ratio between the fluids' flow rates gov-

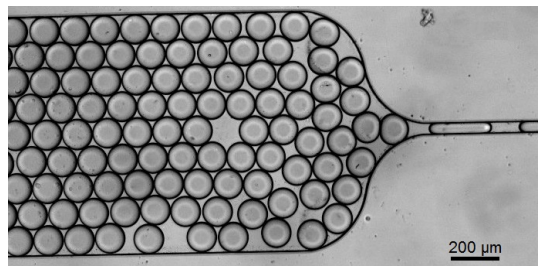

Figure 8.2: Dropelt generation in a microfluidic device. Here are water droplets generated in oil. Scale bar is 200 μm.

ern the size of the droplets; if the ratio is defined as $\frac{Q_{water}}{Q_{oil}}$ lower values will result in smaller droplets and bigger values will result in bigger droplets. Additional, while keeping the flow rate ratio constant an increased total flow rate of the fluids resulted in smaller droplets. Next, different concentrations of added surfactants affected the droplet size - with higher concentrations the droplet diameter decreased. This is due to the decreasing surface tension between the fluids with increasing surfactant concentration. The tested concentrations were 1, 2 and 4 % (volume/volume) of added surfactants to the oil. If no surfactants were added the droplets weren't stable and coalescence occurred when droplets encountered each other. Lastly, the channel dimension have shown to govern the droplet size. With smaller dimension smaller droplets are generated compared to wider channels. This due to the higher flow rates in the smaller channels that increases the shear rate in the system. With bigger shear rates smaller droplets are formed.

There are many parameters that one has to consider before any applications involving droplets are designed and fabricated. E.g. if the aim is to generate small droplets with low volumes (e.g. in single cell analysis) the channel dimensions has to be small or if larger droplets are desired wider channels could be used. Then can the flow rates of the fluids be determined as well as a suitable surfactant concentration.

Bibliography

[1] George M Whitesides. "The origins and the future of microfluidics". In: *Nature* 442.7101 (2006), pp. 368–373.

[2] Chun-Xia Zhao. "Multiphase flow microfluidics for the production of single or multiple emulsions for drug delivery". In: *Advanced drug delivery reviews* 65.11 (2013), pp. 1420–1446.

[3] Andrew J Demello. "Control and detection of chemical reactions in microfluidic systems." In: *Nature* 442.7101 (2006), pp. 394–402.

[4] Jamil El-Ali, Peter K Sorger, and Klavs F Jensen. "Cells on chips". In: *Nature* 442.7101 (2006), pp. 403–411.

[5] Douglas B Weibel and George M Whitesides. "Applications of microfluidics in chemical biology". In: *Current Opinion in Chemical Biology* 10.6 (2006), pp. 584–591.

[6] Petra S Dittrich, Kaoru Tachikawa, and Andreas Manz. "Micro total analysis systems. Latest advancements and trends". In: *Analytical chemistry* 78.12 (2006), pp. 3887–3908.

[7] Stefan Haeberle and Roland Zengerle. "Microfluidic platforms for lab-on-a-chip applications". In: *Lab on a Chip* 7.9 (2007), pp. 1094–1110.

[8] Jack W Judy. "Microelectromechanical systems (MEMS): fabrication, design and applications". In: *Smart materials and Structures* 10.6 (2001), p. 1115.

[9] Younan Xia and George M Whitesides. "Soft lithography". In: *Annual review of materials science* 28.1 (1998), pp. 153–184.

[10] Samuel K Sia and George M Whitesides. "Microfluidic devices fabricated in poly (dimethylsiloxane) for biological studies". In: *Electrophoresis* 24.21 (2003), pp. 3563–3576.

[11] Linas Mazutis et al. "Single-cell analysis and sorting using droplet-based microfluidics". In: *Nature protocols* 8.5 (2013), pp. 870–891.

[12] Helen Song, Delai L Chen, and Rustem F Ismagilov. "Reactions in droplets in microfluidic channels". In: *Angewandte chemie international edition* 45.44 (2006), pp. 7336–7356.

[13] J Michael Köhler and Thomas Henkel. "Chip devices for miniaturized biotechnology". In: *Applied microbiology and biotechnology* 69.2 (2005), pp. 113–125.

[14] Shia-Yen Teh et al. "Droplet microfluidics". In: *Lab on a Chip* 8.2 (2008), pp. 198–220.

[15] Huei-Wen Wu et al. "Exploitation of a microfluidic device capable of generating size-tunable droplets for gene delivery". In: *Microfluidics and nanofluidics* 7.1 (2009), pp. 45–56.

[16] Yihong Zhan et al. "Electroporation of cells in microfluidic droplets". In: *Analytical chemistry* 81.5 (2009), pp. 2027–2031.

[17] Asami Kubo, Hideyuki Shinmori, and Toshifumi Takeuchi. "Atrazine-imprinted microspheres prepared using a microfluidic device". In: *Chemistry Letters* 35.6 (2006), pp. 588–589.

[18] Henrik Bruus. *Theoretical microfluidics*. Vol. 18. Oxford University Press, 2008.

[19] Nam-Trung Nguyen and Steven T Wereley. *Fundamentals and applications of microfluidics*. Artech House, 2002.

[20] Wikimedia Commons. Accessed: 2014-04-18. URL: `http://http://commons.wikimedia.org/wiki/File:Laminar_and_turbulent_flows.svg`.

[21] Todd M Squires and Stephen R Quake. "Microfluidics: Fluid physics at the nanoliter scale". In: *Reviews of modern physics* 77.3 (2005), p. 977.

[22] Yonghao Zhang and Haihu Liu. "Physics of Multiphase Microflows and Microdroplets." In: *Microdroplet Technology* (2012), p. 1. ISSN: 9781461432647.

[23] Wikimedia Commons. Accessed: 2014-04-18. URL: `http://commons.wikimedia.org/wiki/File:Wassermolek%C3%BCleInTr%C3%B6pfchen.svg`.

[24] Wikimedia Commons. Accessed: 2014-05-11. URL: `http://http://commons.wikimedia.org/wiki/File:Contact_angle.svg`.

[25] Lord Rayleigh. "On the capillary phenomena of jets". In: *Proceedings of the Royal Society of London* 29.196-199 (1879), pp. 71–97.

[26] Jens Eggers. "Nonlinear dynamics and breakup of free-surface flows". In: *Reviews of modern physics* 69.3 (1997), p. 865.

[27] Charles N Baroud, Francois Gallaire, and Rémi Dangla. "Dynamics of microfluidic droplets". In: *Lab on a Chip* 10.16 (2010), pp. 2032–2045.

[28] Todd Thorsen et al. "Dynamic pattern formation in a vesicle-generating microfluidic device". In: *Physical review letters* 86.18 (2001), p. 4163.

[29] M De Menech et al. "Transition from squeezing to dripping in a microfluidic T-shaped junction". In: *Journal of Fluid Mechanics* 595 (2008), pp. 141–161.

[30] Haihu Liu and Yonghao Zhang. "Droplet formation in a T-shaped microfluidic junction". In: *Journal of applied physics* 106.3 (2009), p. 034906.

[31] AS Utada et al. "Dripping, jetting, drops, and wetting: the magic of microfluidics". In: *Mrs Bulletin* 32.09 (2007), pp. 702–708.

[32] Carsten Cramer, Peter Fischer, and Erich J Windhab. "Drop formation in a co-flowing ambient fluid". In: *Chemical Engineering Science* 59.15 (2004), pp. 3045–3058.

[33] Shelley L Anna, Nathalie Bontoux, and Howard A Stone. "Formation of dispersions using flow focusing in microchannels". In: *Applied physics letters* 82.3 (2003), pp. 364–366.

[34] Remi Dreyfus, Patrick Tabeling, Herve Willaime, et al. "Ordered and disordered patterns in two-phase flows in microchannels". In: *Physical review letters* 90.14 (2003), pp. 144505–144505.

[35] Ralf Seemann et al. "Droplet based microfluidics". In: *Reports on progress in physics* 75.1 (2012), p. 016601.

[36] C Holtze et al. "Biocompatible surfactants for water-in-fluorocarbon emulsions". In: *Lab on a Chip* 8.10 (2008), pp. 1632–1639.

[37] 3M distibutor ACOTA. Accessed: 2014-05-22. URL: `http://www.acota.co.uk/products/Novec-Fluids`.

[38] A Abrishamkar et al. *A COMSOL Multiphysics® Model of Droplet Formation at a Flow Focusing Device*. URL: `http://www.comsol.it/conference2013/europe/abstract/id/16265/abrishamkar_abstract.pdf`.

[39] Hongbin Yu et al. "Soft lithography replication based on PDMS partial curing". In: *Microsystem technologies* 17.3 (2011), pp. 443–449.

[40] Shantanu Bhattacharya et al. "Studies on surface wettability of poly (dimethyl) siloxane (PDMS) and glass under oxygen-plasma treatment and correlation with bond strength". In: *Microelectromechanical Systems, Journal of* 14.3 (2005), pp. 590–597.

[41] Dhananjay Dendukuri et al. “Controlled synthesis of nonspherical microparticles using microfluidics”. In: *Langmuir* 21.6 (2005), pp. 2113–2116.

[42] Dolomite Microfluidics. Accessed: 2014-05-20. URL: http://www.dolomite-microfluidics.com/webshop/droplet_systems_1.

[43] Nicholas J Douville et al. “Fabrication of two-layered channel system with embedded electrodes to measure resistance across epithelial and endothelial barriers”. In: *Analytical chemistry* 82.6 (2010), pp. 2505–2511.

[44] Sigma-Aldrich. Accessed: 2014-05-12. URL: http://www.sigmaaldrich.com/catalog/product/sigma/ge17133201?lang=en&region=SE.

[45] MicroChemicals. Accessed: 2014-05-19. URL: http://www.microchemicals.com/micro/az_125nxt_photoresist.pdf.

[46] Haihu Liu and Yonghao Zhang. “Droplet formation in microfluidic cross-junctions”. In: *Physics of Fluids (1994-present)* 23.8 (2011), p. 082101.

[47] Yung-Chieh Tan, Vittorio Cristini, and Abraham P Lee. “Monodispersed microfluidic droplet generation by shear focusing microfluidic device”. In: *Sensors and Actuators B: Chemical* 114.1 (2006), pp. 350–356.

[48] J Tan et al. “Drop dispenser in a cross-junction microfluidic device: Scaling and mechanism of break-up”. In: *Chemical Engineering Journal* 136.2 (2008), pp. 306–311.

[49] Shelley L Anna and Hans C Mayer. “Microscale tipstreaming in a microfluidic flow focusing device”. In: *Physics of Fluids (1994-present)* 18.12 (2006), p. 121512.

[50] Haakan N Joensson, Mathias Uhlén, and Helene Andersson Svahn. “Droplet size based separation by deterministic lateral displacementseparating droplets by cell-induced shrinking”. In: *Lab on a Chip* 11.7 (2011), pp. 1305–1310.

[51] Su-Kyoung Chae et al. “Oil droplet generation in PDMS microchannel using an amphiphilic continuous phase”. In: *Lab on a Chip* 9.13 (2009), pp. 1957–1961.

Appendices

Appendix A

Photolithograpic Masks

A.1 First Mask

The figures below are cropped from the original mask-drawing, due to that the small features would not be visible.

AI

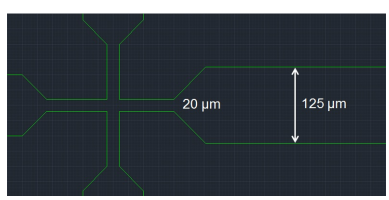

AII

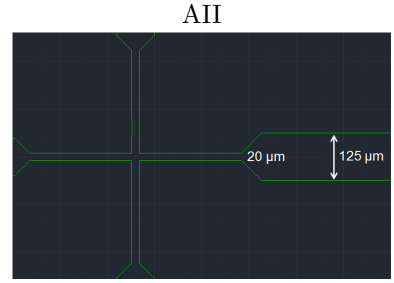

AIII

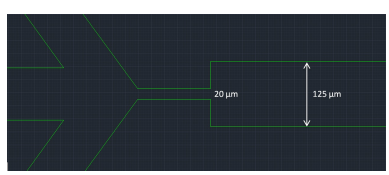

AIV

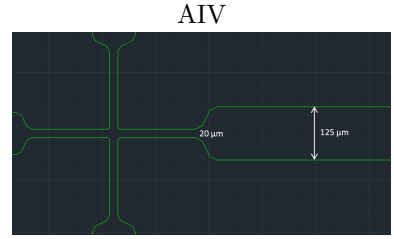

AV

AVI

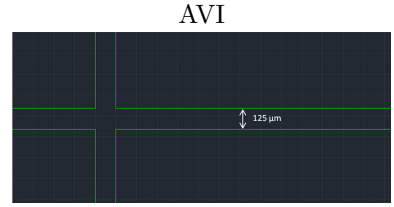

BI

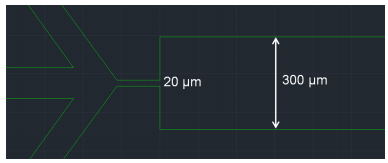

BII

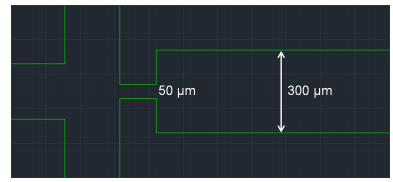

BIII

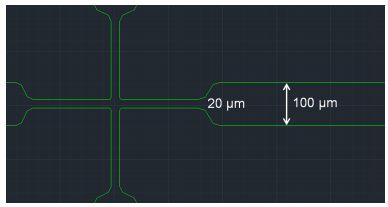

BIV

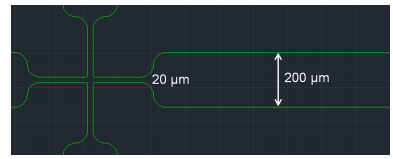

BV

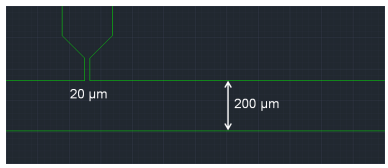

Inlets & Outlets

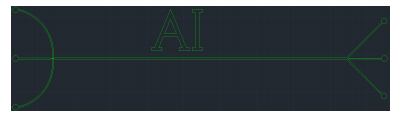

A.2 Second Mask

CI

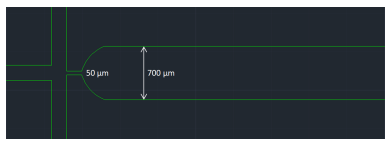

CII

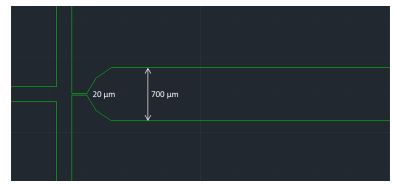

DI

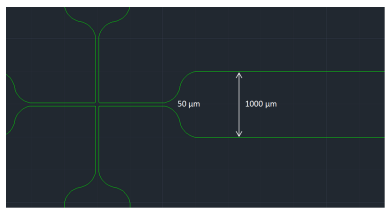

DII

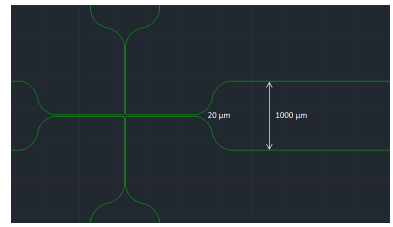

EI

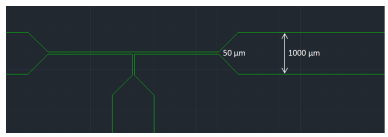

Reducing Inlets

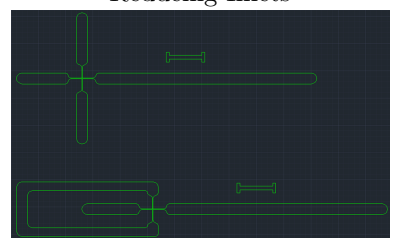

Appendix B

Defect Devices

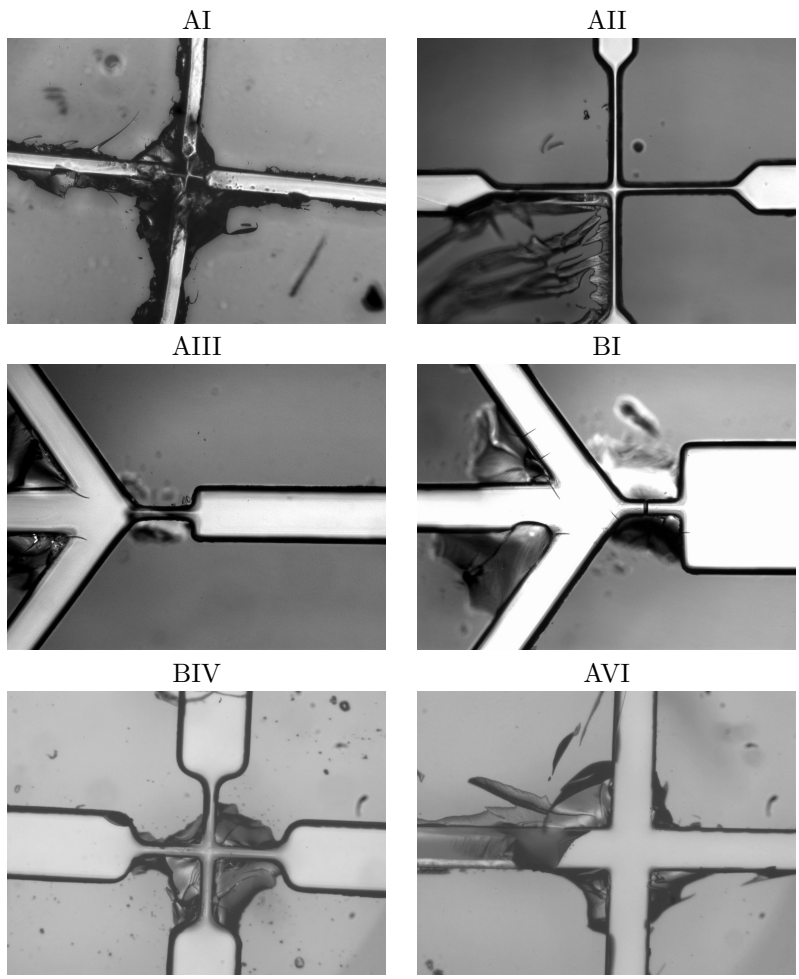

Figures of some defect devices, due to the PDMS detachment from master were not successful.

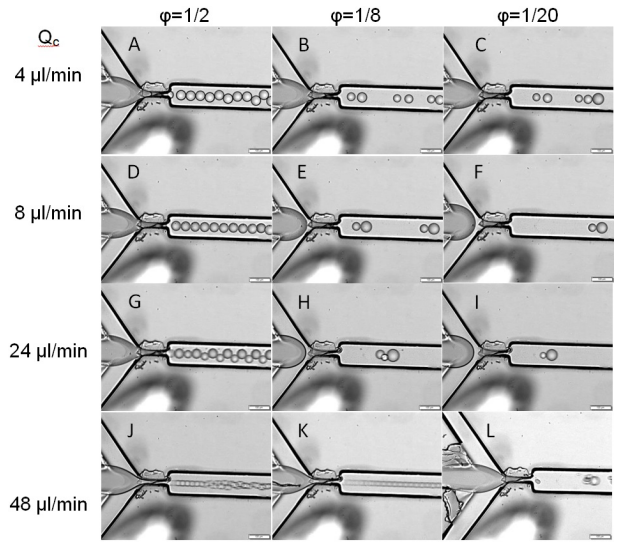

Figures of a defect device, of the *AIII* design, where different flow rates and flow rate ratios were tested. Polydisperse droplets can be seen in (B), (C), (E) - (I) and (L), Monodisperse droplets can be seen (A), (D), (J) and (K). Scale bar is 200 μm.

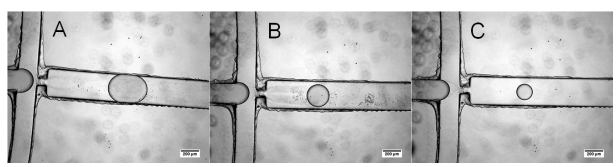

Figures of a defect device, of the *DII* design, where flow rate ratio dependency was tested. Plugs are formed in (A), while droplets are generated in (B) and (C). Scale bar is 200 μm

Appendix C

Instrumentation

Software

Drawing photolithographic mask: AutoCAD® 2013 (Autodesk)
Simulations: COMSOL Multiphysics®
Computer software controlling pumps: neMESYS UserInterface Software
Computer Software for camera: cellSens®

Fabrication

Photoresist: AZ-125nXT-10A (Micro Chemicals)
Developer: AZ 326 (Micro Chemicals)
Photosensitive film: SuperPHAT, 100 μm and 400 μm (Chromaline)
Silicone rubber: Polydimethylsiloxane (PDMS), Sylgard 184 (Sigma-Aldrich)

Fluids

Continuous phase: Novec 7500, 3-ethoxy-1,1,1,2,3,4,4,5,5,6,6,6-dodecafluoro-2-trifluoromethyl-hexane (3M)
Dispersed phase: MilliQ water
Surfactants: Krytox, poly(perfluoropropylene glycol)-carboxylate (DuPont)
Surface treatment: Repel-Silane, Dimethyldichlorosilane (PlusOne)

Equipment

Syringe pumps: neMESYS (Cetoni)
Syringes: Plastic syringes, 1 ml (BD)
Microscope: BX51WI (Olympus)
Camera: CAM-XM10 (Olympus)
Tubings: TFE Teflon® Tubing, 1.58 mm OD x 0.3 mm ID

Appendix D

Protocols

D.1 Master fabrication

Spinner

1. Set the hot plate to 135 °C.
2. Set the spinning program to the following setup:
   (a) 1100 RPM, 5000 RPM/s, 4 seconds
   (b) 500 RPM, 5000 RPM/s, 30 seconds
   (c) end
3. Attach wafer to the spinner then make sure it is fixed by vacuum.
4. Apply roughly 2 ml photoresist in the middle of the wafer.
5. Start the spinning program, after it is finished let the wafer stay for 5 minutes, for any roughness of the resist to be smoothed.
6. Place the wafer on the hot plate for 25 min.

Lithography

1. Mount the wafer in the aligner, make sure it is fixed by vacuum.
2. Mount the photomask in the aligner.
3. Align the wafer and mask, and set them in contact. (Soft contact was used between the wafer and the mask since no vacuum contact could be applied. However, vacuum contact is preferred.)
4. Expose by UV-light for 7x60 seconds.

Development

1. Prepare two cups with developer and two cups with MilliQ water.
2. Develop the resist in the first cup with developer for 60 seconds.
3. Rinse the wafer in MilliQ water for 60 seconds.
4. Repeat the development and rinsing additionally two times.
5. Develop any remaining resist in the second cup with developer for 60 seconds at a time with 60 seconds of rinsing in MilliQ in between. Repeat until all unwanted resist are gone.
6. Do a final rinse in the second cup with water.
7. Blow dry with nitrogen gas.

D.2 Device fabrication

The fabrication of the device consists of the four steps presented below, then is the device ready for use.

Master Silanization

Silanize the surface of the master with Repel-Silane. Apply a few drops of Repel-Silane next to the master and let the solution evaporate in a desiccator. This will create a self-ordered monolayer of dimethyldichlorosilane on the master, which will facilitate the removal of PDMS. To enhance the binding of Repel-Silane the surface can be activated by oxygen plasma treatment with Oxygen can be performed to activate the surface of the master, however, this was not needed in our case.

PDMS

1. Prepare PDMS with base and curing agent to a ratio of 10:1, mix for a few minutes.
2. Pour PDMS on the master, and put let desiccate in a desiccator for 30-45 minutes, release the under pressure every 10-15 minutes to blast the air bubbles in the PDMS.
3. Put the master with the PDMS in 60 °C for two hours.

PDMS-glass bonding

1. Dice the PDMS slabs and gently release them from the master stamp.
2. Make holes in the PDMS slabs for TFE tubings using a syringe needle.
3. Clean glass slides with acetone and ethanol
4. Expose PDMS + glass slide to UV-Ozone for 10 minutes. NB! Bonding surface should be placed facing upwards in the UV-Ozone machine.

5. Place PDMS and glass slide in contact. Push out any trapped air.
6. Place the PDMS and glass slide in 70 °C for 30 minutes for thermal bonding.

Lastly, glue rubber tubings (1/16 in ID x 1/8 in OD), approx. 5 - 6 mm long, to the holes previously made in the PDMS slabs and let cure. TFE tubings are then inserted into the rubber tubes for tight sealing.

Channel surface treatment

To make the channel inner walls hydrophobic Repel-Silane was used once again. PDMS is by itself hydrophobic but the glass slide is hydrophilic, hence the treatment is necessary.

1. Fill the device with Repel-Silane with a syringe and make sure the main duct is completely filled. Let stay for 5-10 minutes for the chemical binding to occur.
2. Flush the device with air to remove the remaining solution, then put the device in a desiccator for 30 minutes.
3. Fill the channel with the continuous phase.

Appendix E

Abstract to MSW 2014

Abstract contribution to MicroNano System Workshop 2014 (MSW 2014) at Uppsala University, 15-16 may 2014.

DEVELOPMENT OF A DROPLET GENERATOR TOWARDS APPLICATIONS USING ACOUSTOPHORETIC SORTING

Linus Jonsson[1], Anna Fornell[1], Haakan Joensson[2], Johan Nilsson[1], Maria Tenje[1]

[1] Department of Biomedical Engineering
Lund University
S-221 00 Lund, Sweden

[2] Div of Proteomics and Nanobiotechnology
Royal Institute of Technology (KTH), Science for Life Laboratory
Box 1031
S-171 21 Solna, Sweden

E-mail: maria.tenje@elmat.lth.se

Background

The generation and use of microdroplets of two immiscible liquids in microfluidics system have shown great potential in many scientific fields; for fast analytical system, precise and controllable reactions, multiple or single cell analysis, material synthesis, protein crystallization and for fabrication of micro- and nano particles [1] [2]. The small volume of the generated droplets and the extreme generation rate results in higher through-put and lowers the costs compared to conventional macro-scale systems [3] [4]. One issue is how to sort the droplets of interest from the continuous phase. One approach to sort the droplets in a microfluidic device could be to utilize acoustophoresis [5]. Here we present the work done to fabricate a device for droplet generation that in the future could be coupled with acoustophoresis.

Experimental methods

A master mold was created by standard soft photolithography. First the negative photoresist (AZ 125nXT-10A, MicroChemicals) was spin-coated on a silicon wafer. After exposure to UV-light the unexposed resist was developed (AZ 326 Developer, MicroChemicals). Then PDMS (SYLGARD 184, SIGMA-ALDRICH), base and curing agent was mixed in the ratio 10:1, poured over the master and heated at 80 °C for 60 minutes for cross-linking to occur. The cured PDMS was then peeled off from the master and bonded on a 1 mm thick microscope glass slide (UV/Ozone-treatment on the bonding surfaces) and thermally bonded in 70 °C for 30 minutes. Holes were made in the PDMS for attachment of tubings using a syringe needle. The internal channel walls were silanized (Repel Silane-ES, Pharmacia Biotech) for 10 minutes then completely dried in a vacuum chamber.

One of the devices fabricated have the following dimensions; width is 125 µm, width at orifice is 20 µm and the height is around 90-100 µm, see Figure 1.

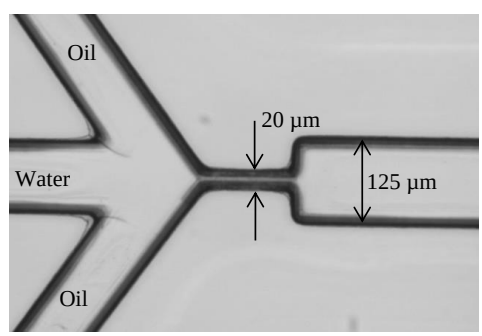

Figure 1. Microscopic picture of the master fabricated by standard photolithography, 5x magnification.

As the continouos phase we used fluorinated oil (Novec 7500, 3M) with 2% v/v surfactant (Krytox, DuPont). As the discrete phase we used MQ-water with 0.025% v/v Triton X-100 (Sigma-Aldrich) The fluids were injected to the device by syringe pumps (neMESYS, Cetoni). The droplet generation was observed and recorded in a microscope with a mounted camera (CAM-XM10, Olympus). We

studied how the droplet size and generation rate altered by varying the flow rates and the flow ratios of the two fluids.

COMSOL simulations were performed to demonstrate the effect of varying flow rates and flow ratios in a theoretical manner. The simulations were, for the sake of time, made in 2D and the velocities were chosen arbitrarily whereas the ratio between the two flows was always 2:1. The fluid properties of water were used for the discrete phase (density 1e3 kg/m^3 and dynamic viscosity 1e-3 Pas) and of Novec 7500 as the continuous phase (density 1600 kg/m^3 and dynamic viscosity 1.24e-3 Pas). Interfacial surface tension between the two phases was set to 16e-3 N/m, wall properties; wetted wall – contact angle: -π/9, which will simulate that the continuous phase wets the channels and the droplets formed inside will not wet the channel.

Results

By varying the fluid flows and the flow ratios of oil:water, the droplet size and generation rates changed. In the experiments shown in Table 1, monodisperse suspensions of water droplets in oil were achieved for flow settings in A, D, J, and K. The settings in B, E, F, G and I generated bidisperse droplets and in C, H and L generated polydisperse droplets. The results show that successful generation of monodisperse droplets is dependent on both flow ratio and total flow rate. The best performance seems to be at low flow ratios since monodisperse and non-pulsing droplets were formed. The volumes of the droplets range from 4 pl to 110 pl.

Table 1. Phase diagram of droplet formation at different flows and ratios. Scale bar: 100 µm in all images.

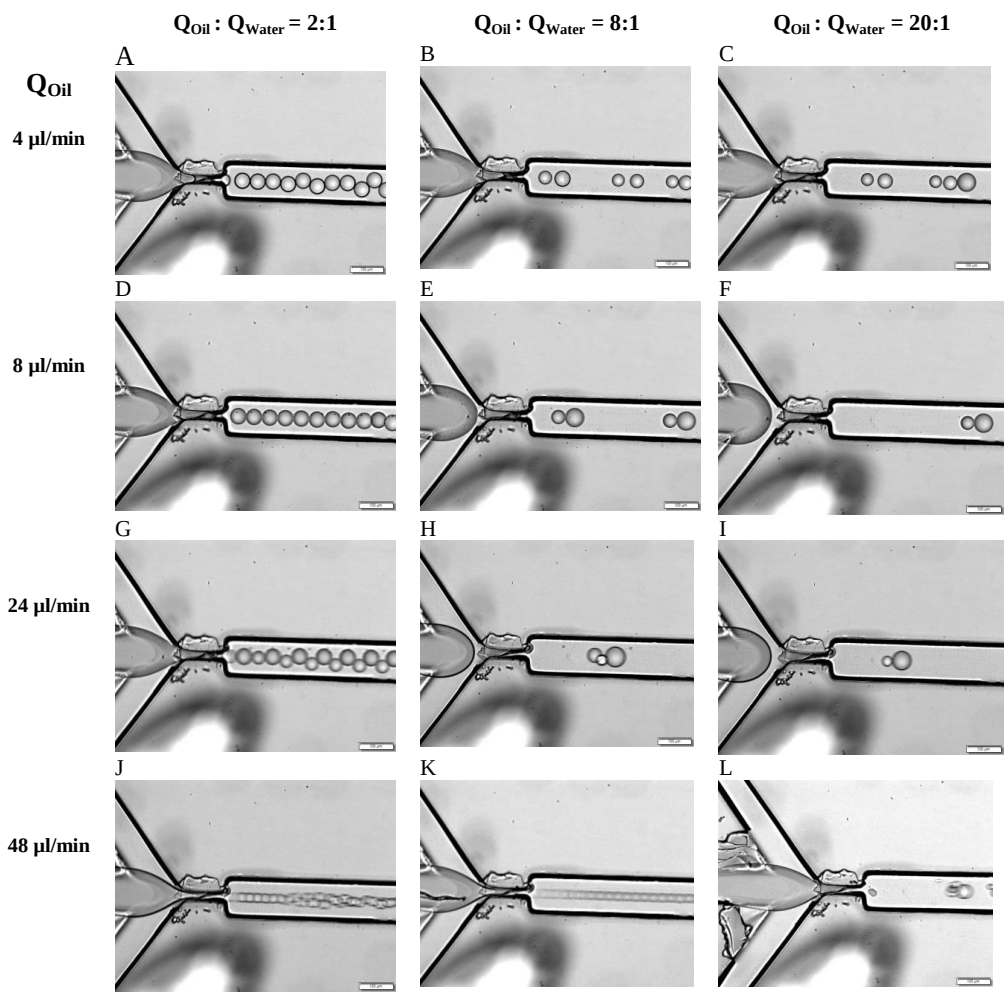

The COMSOL simulation also shows that the flow ratio of the two fluids gives different formation of droplets at different flows, see Table 2. The geometry of the device used in the simulations is slightly different from the fabricated device, to simplify the simulation as a first approximation. The flow ratio is set as 2:1 between the continuous and the discrete phases and the flow velocities are varied from 0.02 m/s to 0.12 m/s. By looking at the simulation one can see that the droplet formation changes also depending on the velocities and not only depending on different flow ratios. In the simulations we saw that for low velocities it is better with low ratios between the continuous and discrete phase while with increased velocity bigger ratios between the phases are required for droplet formation. The simulations are not directly comparable with the experimental work since the design and dimensions in the COMSOL model is not the same as in the experimental device. This is due to the orifice in the COMSOL design is 50 µm and the width of the channel is 200 µm, and the interfacial surface tension may differ from the experimental value. However, one thing the simulation has in common with the experiment is that the size of the droplet decreases with increasing flow rate.

As a conclusion, one must accurately choose the total flow rates and flow ratios to get stable and monodisperse droplets of the desired size and rate for the applications.

Table 2. Diagram of COMSOL simulation demonstrating the different droplet formation at varying flows, ratio is kept at 2:1. The velocity of 0.02 m/s and 0.12 m/s is comparable to the experimental flows of 8 µl/min and 48µl/min, respectively.

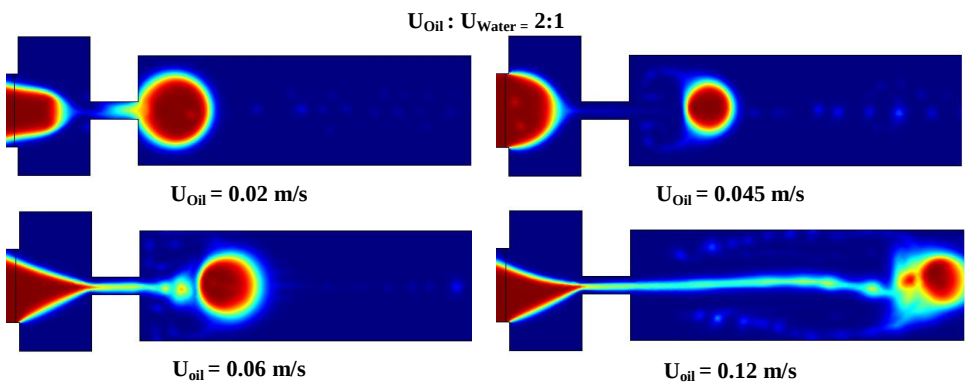

Potential applications

Next step is to combine the droplet generating chip with acoustophoresis to investigate the possibilities to sort the droplets with possible applications of sorting droplets in a microsystem for directed evolutionary studies [6].

REFERENCES

[1] Umbanhowar P. B., Prasad V., Weitz D.A., "Monodisperse emulsion generation via drop break off in a coflowing stream", *Langmuir*, vol. 16, pp. 347-351, 2000

[2] Thorsen T., Roberts R. W., Arnold F. H., Quake S. R., "Dynamic pattern formation in a vesicle-generating microfluidic device", *Physical Review Letters*, vol. 86(18), pp. 4163-4166, 2001

[3] Huebner, A., Sharma, S., Srisa-Art, M., Hollfelder, F., Edel, J., & Demello, A.,"Microdroplets: A sea of applications?", *Lab On A Chip*, vol. 8(8), pp. 1244-1254, Aug 2008

[4] Seemann, R., Brinkmann, M., Pfohl, T., & Herminghaus, S., "Droplet based microfluidics", *Reports On Progress In Physics*, vol. 75(1), 2012

[5] Laurell, T., Petersson F., Nilsson A., "Chip integrated strategies for acoustic separation and manipulation of cells and particles", *Chemical Society Reviews*, vol. 36, pp. 492-506, 2007

[6] Sjostrom S. L., Bai Y., Huang M., Liu Z., Nielsen J., Joensson H. N., Andersson Svahn H., "High-throughput screening for industrial enzyme production hosts by droplet microfluidics", *Lab On A Chip*, vol. 14, pp. 806-813, 2014